15. **Halgren, T. A.** 1996. Merck molecular force field. I. Basis, form, scope, parameterization, and performance of MMFF94. J. Comput. Chem. **17**:490–519.
16. **Hatada, M., K. Yoshimura, S. Harada, J. Shibata, and S. Matsushita.** 2010. HIV-1 evasion of a neutralizing anti-V3 antibody involves acquisition of a potential glycosylation site in V2. J. Gen. Virol. **91**:1335–1345.
17. **Hope, T. J., X. J. Huang, D. McDonald, and T. G. Parslow.** 1990. Steroid-receptor fusion of the human immunodeficiency virus type 1 Rev transactivator: mapping cryptic functions of the arginine-rich motif. Proc. Natl. Acad. Sci. U. S. A. **87**:7787–7791.
18. **Johnson, W. E., and R. C. Desrosiers.** 2002. Viral persistence: HIV's strategies of immune system evasion. Annu. Rev. Med. **53**:499–518.
19. **Kimura, T., K. Yoshimura, K. Nishihara, Y. Maeda, S. Matsumi, A. Koito, and S. Matsushita.** 2002. Reconstitution of spontaneous neutralizing antibody response against autologous human immunodeficiency virus during highly active antiretroviral therapy. J. Infect. Dis. **185**:53–60.
20. **Kwong, P. D., R. Wyatt, J. Robinson, R. W. Sweet, J. Sodroski, and W. A. Hendrickson.** 1998. Structure of an HIV gp120 envelope glycoprotein in complex with the CD4 receptor and a neutralizing human antibody. Nature **393**:648–659.
21. **Lu, M., S. C. Blacklow, and P. S. Kim.** 1995. A trimeric structural domain of the HIV-1 transmembrane glycoprotein. Nat. Struct. Biol. **2**:1075–1082.
22. **Lusso, P., P. L. Earl, F. Sironi, F. Santoro, C. Ripamonti, G. Scarlatti, R. Longhi, E. A. Berger, and S. E. Burastero.** 2005. Cryptic nature of a conserved, CD4-inducible V3 loop neutralization epitope in the native envelope glycoprotein oligomer of CCR5-restricted, but not CXCR4-using, primary human immunodeficiency virus type 1 strains. J. Virol. **79**:6957–6968.
23. **Madani, N., A. Schon, A. M. Princiotto, J. M. Lalonde, J. R. Courter, T. Soeta, D. Ng, L. Wang, E. T. Brower, S. H. Xiang, Y. D. Kwon, C. C. Huang, R. Wyatt, P. D. Kwong, E. Freire, A. B. Smith III, and J. Sodroski.** 2008. Small-molecule CD4 mimics interact with a highly conserved pocket on HIV-1 gp120. Structure **16**:1689–1701.
24. **Maeda, Y., K. Yusa, and S. Harada.** 2008. Altered sensitivity of an R5X4 HIV-1 strain 89.6 to coreceptor inhibitors by a single amino acid substitution in the V3 region of gp120. Antivir. Res. **77**:128–135.
25. **Schön, A., N. Madani, J. C. Klein, A. Hubicki, D. Ng, X. Yang, A. B. Smith III, J. Sodroski, and E. Freire.** 2006. Thermodynamics of binding of a low-molecular-weight CD4 mimetic to HIV-1 gp120. Biochemistry **45**:10973–10980.
26. **Shibata, J., K. Yoshimura, A. Honda, A. Koito, T. Murakami, and S. Matsushita.** 2007. Impact of V2 mutations on escape from a potent neutralizing anti-V3 monoclonal antibody during in vitro selection of a primary human immunodeficiency virus type 1 isolate. J. Virol. **81**:3757–3768.
27. **Thali, M., J. P. Moore, C. Furman, M. Charles, D. D. Ho, J. Robinson, and J. Sodroski.** 1993. Characterization of conserved human immunodeficiency virus type 1 gp120 neutralization epitopes exposed upon gp120-CD4 binding. J. Virol. **67**:3978–3988.
28. **Wang, F. X., T. Kimura, K. Nishihara, K. Yoshimura, A. Koito, and S. Matsushita.** 2002. Emergence of autologous neutralization-resistant variants from preexisting human immunodeficiency virus (HIV) quasispecies during virus rebound in HIV type 1-infected patients undergoing highly active antiretroviral therapy. J. Infect. Dis. **185**:608–617.
29. **Wyatt, R., P. D. Kwong, E. Desjardins, R. W. Sweet, J. Robinson, W. A. Hendrickson, and J. G. Sodroski.** 1998. The antigenic structure of the HIV gp120 envelope glycoprotein. Nature **393**:705–711.
30. **Yamada, Y., C. Ochiai, K. Yoshimura, T. Tanaka, N. Ohashi, T. Narumi, W. Nomura, S. Harada, S. Matsushita, and H. Tamamura.** 2010. CD4 mimics targeting the mechanism of HIV entry. Bioorg. Med. Chem. Lett. **20**:354–358.
31. **Yoshimura, K., R. Kato, M. F. Kavlick, A. Nguyen, V. Maroun, K. Maeda, K. A. Hussain, A. K. Ghosh, S. V. Gulnik, J. W. Erickson, and H. Mitsuya.** 2002. A potent human immunodeficiency virus type 1 protease inhibitor, UIC-94003 (TMC-126), and selection of a novel (A28S) mutation in the protease active site. J. Virol. **76**:1349–1358.
32. **Yoshimura, K., R. Kato, K. Yusa, M. F. Kavlick, V. Maroun, A. Nguyen, T. Mimoto, T. Ueno, M. Shintani, J. Falloon, H. Masur, H. Hayashi, J. Erickson, and H. Mitsuya.** 1999. JE-2147: a dipeptide protease inhibitor (PI) that potently inhibits multi-PI-resistant HIV-1. Proc. Natl. Acad. Sci. U. S. A. **96**:8675–8680.
33. **Yoshimura, K., J. Shibata, T. Kimura, A. Honda, Y. Maeda, A. Koito, T. Murakami, H. Mitsuya, and S. Matsushita.** 2006. Resistance profile of a neutralizing anti-HIV monoclonal antibody, KD-247, that shows favourable synergism with anti-CCR5 inhibitors. AIDS **20**:2065–2073.
34. **Yusa, K., Y. Maeda, A. Fujioka, K. Monde, and S. Harada.** 2005. Isolation of TAK-779-resistant HIV-1 from an R5 HIV-1 GP120 V3 loop library. J. Biol. Chem. **280**:30083–30090.
35. **Zhao, Q., L. Ma, S. Jiang, H. Lu, S. Liu, Y. He, N. Strick, N. Neamati, and A. K. Debnath.** 2005. Identification of *N*-phenyl-*N'*-(2,2,6,6-tetramethyl-piperidin-4-yl)-oxalamides as a new class of HIV-1 entry inhibitors that prevent gp120 binding to CD4. Virology **339**:213–225.

Journal of General Virology (2010), **91**, 1335–1345 DOI 10.1099/vir.0.017426-0

Human immunodeficiency virus type 1 evasion of a neutralizing anti-V3 antibody involves acquisition of a potential glycosylation site in V2

Makiko Hatada, Kazuhisa Yoshimura, Shigeyoshi Harada, Yoko Kawanami, Junji Shibata and Shuzo Matsushita

Correspondence
Shuzo Matsushita
shuzo@kumamoto-u.ac.jp

Division of Clinical Retrovirology and Infectious Diseases, Center for AIDS Research, Kumamoto University, Kumamoto 860-0811, Japan

It has been reported that the addition of a potential *N*-linked glycosylation site (PNGS) to the gp120 human immunodeficiency virus type 1 (HIV-1) envelope glycoprotein provides protection against neutralizing antibodies (NAbs) by acting as a 'glycan shield'. In this study, we induced insertion of a PNGS into the V2 region of HIV-1_{BaL} with the KD-247 anti-V3 neutralizing monoclonal antibody. In the presence of KD-247 (200 μg ml^{-1}) at passage five, viruses with 3 aa mutations in the C2 (T240S and I283T) and V3 (T319A) regions expanded from pre-existing variants. After six passages with KD-247 (>300 μg ml^{-1}), a PNGS emerged in the V2 region in addition to C2 (T240S) and V3 mutations (R315K and F317L). A variant with a PNGS insertion in V2, but no V3 mutations was sensitive to KD-247, whereas a clone with a V2 PNGS insertion and mutations in V3 demonstrated a high level of resistance to KD-247. Replication kinetic analysis revealed that the F317L mutation in V3 played a compensatory role for fitness-loss caused by the PNGS insertion in V2. The evading HIV-1 variant did not revert back to the wild-type virus after 14 passages without KD-247. These findings demonstrate that the virus with fitness-loss mutations can replicate equally as well as the wild-type virus to acquire some key mutations in the V3 stem and the C2 region, and the compensated variants containing PNGS do not revert back to the ancestral virus even in the absence of NAb.

Received 7 October 2009
Accepted 18 December 2009

INTRODUCTION

A neutralizing antibody (NAb) against human immunodeficiency virus type 1 (HIV-1) is an essential component of a protective vaccine. However, primary isolates of HIV-1 are relatively resistant to neutralization compared with variants selected for growth in permanent cell lines (Moore *et al.*, 1995; Pugach *et al.*, 2004). Studies addressing differences between neutralization-sensitive and -resistant variants have revealed several mechanisms that are responsible for neutralization resistance in primary isolates. These mechanisms include the occlusion of epitopes within the envelope glycoprotein (Env) oligomer and the extensive glycosylation and extension of variable loops from the surface of the complex leading to steric and conformational blocking of receptor-binding sites (Kwong *et al.*, 2002; McCaffrey *et al.*, 2004; Pinter *et al.*, 2004; Saunders *et al.*, 2005). The structural features of one envelope glycoprotein, Env gp120, mean that it can tolerate a vast array of mutations permitting the selection of neutralization evading variants, as has been previously demonstrated in culture assays, animal models and infected individuals (Johnson & Desrosiers, 2002).

Although there are ample data showing that NAbs can protect against HIV-1 infection *in vitro* and *in vivo*, their activity in infected humans remains controversial (Cao *et al.*, 1995; Deeks *et al.*, 2006; Montefiori *et al.*, 2001; Sullivan *et al.*, 1993). Passive transfer of a combination of broadly neutralizing monoclonal antibodies (mAbs) 2G12, 2F5 and 4E10 in patients during a structured treatment interruption resulted in a significant delay in viral rebound in some patients compared with viral rebound in the absence of these antibodies (Trkola *et al.*, 2005). This would indicate that viral suppression was due to the antiviral activity of the administered antibodies. Subsequent studies addressing the pharmacokinetics of each mAb (Joos *et al.*, 2006), neutralization-resistance mutations (Manrique *et al.*, 2007) and protective neutralization titres *in vivo* (Trkola *et al.*, 2008) using samples from the study further supported the protective effects of NAb *in vivo*.

Clinical studies examining NAbs in primary infections have suggested that the majority of recently infected individuals generate a vigorous antibody response against autologous virus. However, the rapid evolution of HIV in the presence

The GenBank/EMBL/DDBJ accession numbers for the sequences determined in this study are AB521136–AB521148.

A supplementary figure is available with the online version of this paper.

of NAb results in the emergence of evading mutants. As a consequence, at any time during the early stages of HIV infection, NAbs are more likely to recognize the earlier form of the viruses as opposed to the recent variants. Despite evidence of phenotypic resistance, the genetic basis of the mechanism allowing primary viruses to evade NAbs is poorly understood.

Wei *et al.* (2003) found that glycosylation of Env plays an important role in evading neutralization. The evolving 'glycan shield' can sterically block antibody binding without mutation at the antibody-binding site (Wei *et al.*, 2003). Also, insertion of potential *N*-linked glycosylation sites (PNGSs) along with other mutations has been associated with viral evasion of NAbs (Bunnik *et al.*, 2008; Wei *et al.*, 2003). Conversely, Frost *et al.* (2005) reported that viral evasion of NAb correlates to the rate of amino acid substitution rather than changes in glycosylation and insertions or deletions in Env (Frost *et al.*, 2005). This would suggest that the individual contribution of PNGSs to the neutralization sensitivity of HIV-1 depends on the presence of other mutations in the Env sequence. However, the relationship between PNGSs and mutations of NAb resistance has not been investigated because of technical difficulties, resulting from the polyclonal nature of NAbs and the primary isolates used in previous clinical studies. To clarify the genetic mechanisms responsible for evading neutralization, it is important to analyse individual mutations, resulting from neutralization evasion of NAbs in an *in vitro* culture system.

Neutralization evasion from anti-V3 mAbs has been reported and associated with amino acid substitution within the epitope of the V3 loop and outside V3 (Gorny *et al.*, 2004; Masuda *et al.*, 1990; Park *et al.*, 1998; Pinter *et al.*, 2004; Shibata *et al.*, 2007; Yoshimura *et al.*, 2006; Zolla-Pazner, 2004). However, the role(s) of PNGSs in resistance to neutralization is not clear because the induction of PNGSs under neutralizing mAbs pressure *in vitro* has not been reported.

In this study, we obtained evasion mutants harbouring PNGSs in the V2 region and mutations in the C2 and V3 regions, during induction of neutralization evasion mutants from anti-V3 mAb KD-247 in HIV-1_{BaL}. KD-247 is a humanized mAb that demonstrates cross-neutralizing activity against HIV-1 isolates in clade B. The epitope of KD-247 was mapped to 6 aa, IGPGRA, at the tip of the V3 loop (Eda *et al.*, 2006). A series of analyses using viral clones that have corresponding mutations present in evading viruses revealed a mutant that has both a PNGS-insertion in V2 and mutations in V3 along with a highly resistant phenotype to the NAb. However, the mutant requires further mutation to compensate for reduced replication ability. Studies to elucidate replication kinetics indicated that the F317L mutation in V3 and the T240S mutation in C2 play a key role in maintaining resistant mutations in V2 and V3, which were related to the fitness-loss. Our study partially explains the complex nature of the development of neutralization resistance observed in previous clinical studies.

RESULTS

Selection of anti-V3 mAb KD-247 evasion mutants from HIV-1_{BaL}

To select an HIV-1 variant that is able to evade neutralization by KD-247 *in vitro*, we exposed PM1/CCR5 cells to HIV-1_{BaL} and serially passaged the virus in the presence of increasing concentrations of KD-247. PM1/CCR5 cells were highly sensitive to both X4 and R5 HIV-1 infection, displaying prominent syncytia (Yusa *et al.*, 2005). As a control, HIV-1_{BaL} was passaged under the same conditions without mAb to monitor spontaneous changes that occurred in the virus during prolonged PM1/CCR5 cell passage (denoted as passage control). Because HIV-1_{BaL} was sensitive to neutralization by KD-247 with an IC_{50} of 3.8 μg ml^{-1} as determined by an MTT assay (data not shown), the selected virus was initially propagated in the presence of 5 μg KD-247 ml^{-1}. During the course of the selection procedure, the mAb concentration was increased to 2000 μg ml^{-1}. Following five rounds of passage (p5), a viral variant designated HIV-1_{BaL} (200) p5 arose that replicated in the presence of 200 μg KD-247 ml^{-1}. After passage 16, a viral variant designated HIV-1_{BaL} (2000) p16 arose that infected PM1/CCR5 cells efficiently in the presence of 2000 μg KD-247 ml^{-1}. We harvested viruses at six passages (p2, p5, p6, p7, p10 and p16) as well as a baseline virus, HIV-1_{BaL} (0) p0, and a passage control designated HIV-1_{BaL} (0) p10. These viruses were evaluated for their sensitivity to KD-247 by using TZM-bl as target cells (Table 1). The IC_{50} values of KD-247 against HIV-1_{BaL} (0) p0, HIV-1_{BaL} (200) p5, HIV-1_{BaL} (300) p6 and HIV-1_{BaL} (2000) p16 were 0.32 ± 0.2, 5.68 ± 1.48, >100 and >100 μg ml^{-1}, respectively, indicating that HIV-1_{BaL} acquired a resistant phenotype against KD-247 during *in vitro* selection. At passage 5, HIV-1_{BaL}

Table 1. Neutralization sensitivities of passaged variants to KD-247

	Passage no.	KD-247 conc. (μg ml^{-1})	IC_{50} (μg ml^{-1})*
Baseline virus	p0	0	0.32 ± 0.20
Passage control	p10	0	0.09 ± 0.04
KD-247 selection	p2	10	0.54 ± 0.19
	p5	200	5.68 ± 1.48
	p6	300	>100
	p7	400	>100
	p10	1000	>100
	p16	2000	>100

*TZM-bl cells (2×10^4 cells per well) were exposed to 300 $TCID_{50}$ of passage control (p10) or KD-247 selected variants (p2, p5, p6, p7, p10 and p16) in the presence of various concentrations of KD-247 in 96-well flat-bottom microculture plates and incubated for 48 h. The IC_{50} values were determined by using a chemiluminescent assay for β-galactosidase detection. Data shown represent the means ± SD from the results of three independent experiments.

acquired a moderately resistant phenotype and after passage 6 the virus had developed a highly resistant phenotype.

DNA sequence of the envelope region of evasion mutants

To determine the genetic basis of resistance in the variant HIV-1_{BaL} strains, the C1–C4 region of the env gene was amplified from genomic DNA extracted from the infected cells, cloned and sequenced (Fig. 1).

At passage 5, moderately resistant variants with T240S, I283T and T319A mutations were in the majority. However, the proportion of variants decreased gradually as the KD-247 concentration was increased (Fig. 1b and Fig. 2e). This observation suggests that at low concentrations of KD-247, the variants with moderate resistance to the anti-V3 mAb are selected from the pre-existing variants.

Insertion of a PNGS in the V2 region and an amino acid substitution at the V3 tip (R315K) were observed at passages 5 and 6, respectively. Both of these alterations were not evident in the passage control but became dominant at later passages in the presence of higher concentrations of KD-247 (Figs 1 and 2). To examine whether the insertion of a PNGS in the V2 region existed among the baseline HIV-1_{BaL} variants, we sequenced a total of 61 env clones from HIV-1_{BaL} before selection. No PNGS insertion was observed in the V2 region among the baseline clones (Fig. 1). This result indicates that the virus with the PNGS insertion in V2 either did not exist or existed at a very low level within the baseline variants.

Neutralization sensitivities of pseudoviruses that have a mutated env gene

To determine which substitutions were responsible for KD-247 resistance, we constructed chimeric viruses, which contained the representative envelopes of HIV-1_{BaL} (200) p5 and HIV-1_{BaL} (1000) p13 and were designated BaL-STA and BaL-PNGS/SKL, respectively (Fig. 3). Chimeric envelopes were constructed by replacing wild-type sequences with mutated envelope-encoding sequences for V2, C2 and V3 in the HIV-1_{BaL} wild-type (BaL-WT) virus with the resulting viruses designated BaL-PNGS and BaL-SKL. Sensitivity was compared between the BaL-WT and mutant viruses using a single-round neutralization assay. As shown in Fig. 4(a), the V3 mutated pseudoviruses, BaL-SKL and BaL-PNGS/SKL were highly resistant to KD-247 (>2500- and >5500-fold, respectively) compared with wild-type virus, whereas the C2 and V3 mutated virus at passage 5, BaL-STA, was partially resistant (25-fold). The susceptibility of the clone with the PNGS insertion in the V2 region alone (BaL-PNGS) to KD-247 was highly comparable to that for BaL-WT, indicating that this variant is sensitive to KD-247. In contrast, the clone with both the PNGS-insertion in V2 and mutations in V3 had a highly resistant phenotype to the mAb. The IC_{50} value for BaL-PNGS/SKL was slightly higher than for BaL-SKL in three independent experiments, although there was no significant difference between these two clones.

To determine the effect of these KD-247-induced mutations in gp120 to other entry inhibitors, we examined the sensitivities of these chimeric pseudotyped viruses to rsCD4, 2D7 and maraviroc, a CCR5 inhibitor. The IC_{50} values for rsCD4, 2D7 and maraviroc to the chimeric viruses were comparable to those of wild-type virus (Fig. 4b–d).

Analyses of replication kinetics of infectious molecular clones with mutant env

In order to clarify the role of the PNGS insertion during the process of neutralization evasion, we constructed replication-competent viruses with the PNGS in the V2 region and/or mutations in C2 and V3 of gp120 by using pWT/BaL proviral plasmid (Fig. 3; they were designated HX-BaL-X). Using these competent viruses with Env mutations we compared the replication kinetics in the absence of KD-247. As shown in Fig. 5(a), HX-BaL-PNGS containing a PNGS in V2 had low levels of p24 antigen compared with the wild-type clone (HX-BaL-WT), whereas HX-BaL-PNGS/SKL containing a PNGS and mutations in the C2 and V3 regions exhibited a replication rate equivalent to the wild-type and HX-BaL-SKL. We also compared their replication kinetics in the presence of low, moderate and high concentrations of KD-247 (Fig. 5b). High concentrations of KD-247 (2000 $\mu g\ ml^{-1}$) resulted in HX-BaL-PNGS/SKL replicating slightly faster than HX-BaL-SKL. HX-BaL-PNGS demonstrated slightly more efficient replication kinetics than the wild-type in the presence of a low concentration of KD-247 (5 $\mu g\ ml^{-1}$), while there was no difference between the two viruses when KD-247 was used at 50 $\mu g\ ml^{-1}$. These results indicated that viruses harbouring a PNGS in V2 were selected for at low concentrations of KD-247 but at high concentrations of the mAb, variants harbouring the additional V3 mutations outgrew the former variants.

To elucidate which amino acid mutation would compensate for the fitness-loss induced by insertion of a PNGS, we compared the replication kinetics of the infectious clones with individual mutations in addition to the PNGS insertion (Fig. 5c). The variants with the T240S, R315K and F317L mutations (HX-BaL-PNGS/SKL) and F317L mutation (HX-BaL-PNGS/L) exhibited a higher replication rate than HX-BaL-PNGS. On the other hand, viruses containing the T240S or R315K mutation in addition to the PNGS insertion (HX-BaL-PNGS/S or HX-BaL-PNGS/K, respectively) replicated as well as or less efficiently than HX-BaL-PNGS. These results suggest that the replication deficiency of the HIV-1_{BaL} variant with the PNGS in the V2 region was compensated by the F317L mutation in the V3 region. An improvement in replication capacity of HX-BaL-PNGS/K was observed in variants with the additional T240S mutation (Fig. 5c).

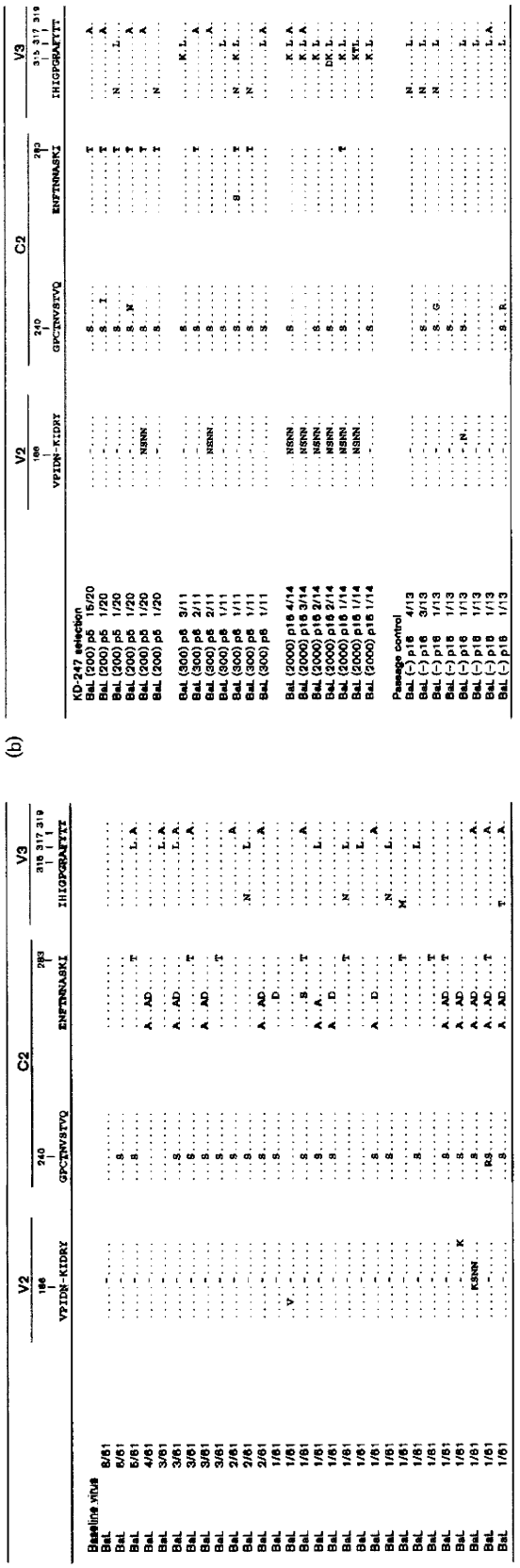

Fig. 1. Amino acid sequences deduced from the nucleotide sequences of env-encoding regions of pDNA isolated at the baseline (a) and indicated passages (p5, p6 and p16) from HIV-1_{BaL} variants selected in the presence of KD-247, and (b) the passage control (p16).The amino acid sequences of the envelope proteins of a clone of HIV-1_{BaL} at baseline are shown at the top as a reference. Identity to the sequence at individual amino acid positions is indicated by dots. The numbers of clones with the given amino acid substitutions among a total of 61 clones (a) and 11–20 clones (b) are listed.

Both the T240S (41/61 clones, 67.2 %) and F317L (18/61, 29.5 %) substitutions were observed in the HIV-1_{BaL} sequence of the baseline viruses. The ratio of threonines and serines at position 240 in gp120 of the passage control remained unchanged at passage 16 (8/13, 61.5 %). The F317L variant in the passage control increased gradually and became more prevalent in the viral population at passage 16 (12/13, 92.3 %) (Fig. 2). These findings suggest that the serine substitution at position 240 in the C2 region of gp120 was required to compensate for inefficient replication rates caused by the R315K and T319A substitutions in the V3 region. Furthermore, the F317L substitution in V3 might play a role in adaptations to survive in PM1/CCR5 cells *in vitro* and also compensate for fitness-loss by the PNGS-insertion in the V2 region induced by KD-247 selection.

Sensitivity of infectious molecular clones containing mutated Env protein to KD-247 and a CCR5 inhibitor

To compare the neutralization sensitivity of the infectious molecular clones, the IC_{50} values were determined for KD-247 by using TZM-bl cells (Table 2). The neutralization sensitivities of clones containing only the PNGS in V2, T240S in C2 and F317L in V3 were virtually the same as the wild-type, whereas the HX-BaL-PNGS/K demonstrated a high level of resistance to KD-247 when compared with HX-BaL-K containing the R315K mutation alone (P=0.006). We constructed a mutant containing an amino acid insertion in V2 without the addition of a glycosylation site and with the R315K mutation (designated HX-BaL-Q/K). The sensitivity of this mutant was comparable to that of the HX-BaL-K mutant (P=0.89). These results taken together suggest that the variant with the PNGS in addition to the R315K mutation in V3 had the highest resistance phenotype to KD-247. We also evaluated sensitivities of these clones to the CCR5 inhibitor, maraviroc. No significant difference was detected for the IC_{50} values of the wild-type and mutant variants to maraviroc.

We then investigated whether the mutations that conferred KD-247 resistance, which were related to a loss in replication efficiency, reverted back to the baseline after several passages in the absence of the anti-V3 mAb. Two mutations, F317L and R315K in the V3 region, the PNGS in the V2 and the T240S mutation in C2 remained dominant in the popu-

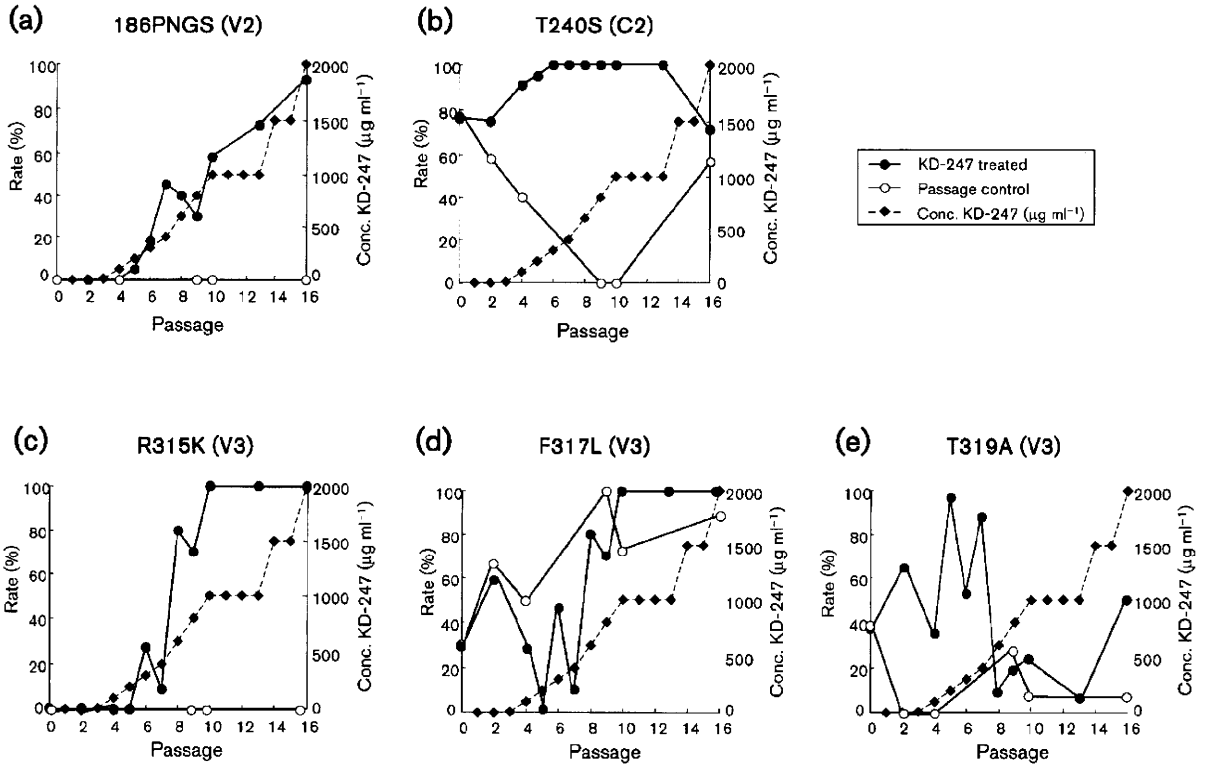

Fig. 2. The gp120 mutation profile of HIV-1_{BaL} evasion variants from KD-247 *in vitro*. The ratio of the PNGS insertion in the V2 region and mutations in the C2 and V3 regions in gp120 of HIV-1_{BaL} variants were plotted for each passage. The *y*-axis indicates the percentage of PNGS insertions or mutations in the tested clones and the *x*-axis shows the concentration of KD-247 (μg ml^{-1}).

lation of viruses that were adept at evasion after culturing for 16 passages in the presence of KD-247 and an additional 14 passages without KD-247 (Fig. 6). The T319A mutation was observed in 90% of clones sequenced at passage 19. However, the frequency of this mutation gradually decreased thereafter (Fig. 6e). These findings show that after acquisition of the mutations in order to compensate for fitness-loss, the HIV-1 variants did not revert back to the wild-type after 14 passages without KD-247.

DISCUSSION

HIV-1 evolution in relation to evasion of humoral immunity has been observed in the early stages of HIV-1

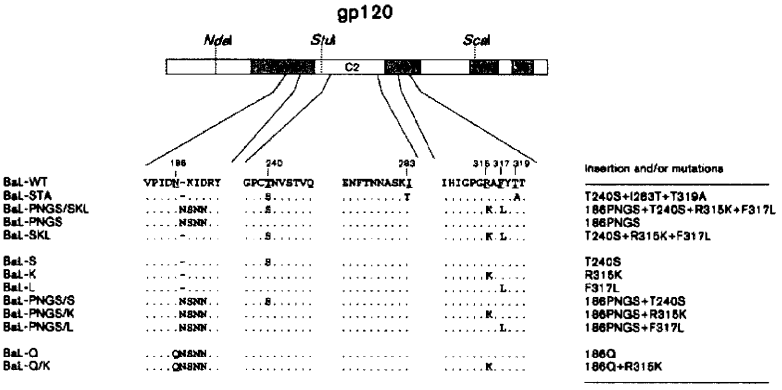

Fig. 3. Schematic representation of recombinant HIV-1_{BaL} env genes used for analysis of the genetic basis for resistance to KD-247. Mutated env genes were amplified from passaged HIV-1_{BaL} virus-infected PM1/CCR5 cells in the absence or presence of KD-247. The recombinant env genes were constructed by replacing each region of passaged control with corresponding sequence of escaped variant of HIV-1_{BaL} or by site-directed mutagenesis. The locations and numbers of specific amino acids, based on the HXB2 sequence, are shown above the reference HIV-1_{BaL} sequence.

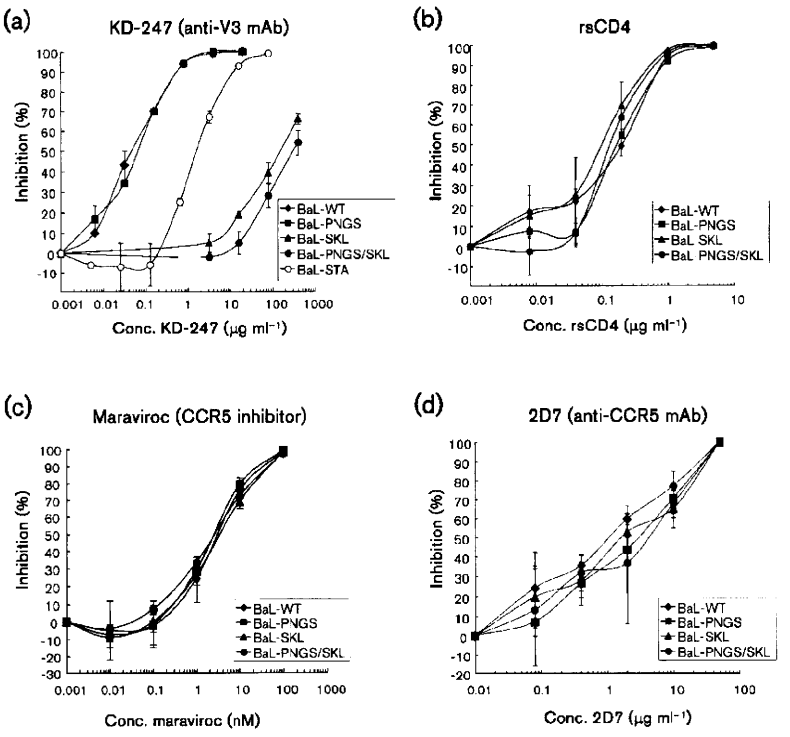

Fig. 4. Sensitivities of HIV-1 strains pseudotyped with recombinant HIV-1_{BaL} env genes to KD-247, 2D7, rsCD4 and CCR5 inhibitor. KD-247, 2D7 (anti-CCR5 mAb), rsCD4 and maraviroc (CCR5 inhibitor) were pre-incubated with 300 $TCID_{50}$ of each HIV-1_{BaL} pseudotype virus for 30 min, then added to TZM-bl target cells. Inhibitory effects were determined by measuring β-galactosidase activity on day 2 of culture.

infection and has been suggested to act as a driving force for the establishment of viral quasispecies *in vivo* (Bunnik *et al.*, 2008; Frost *et al.*, 2005; Mahalanabis *et al.*, 2009; Richman *et al.*, 2003; Wei *et al.*, 2003). In response to NAb pressure, the numbers and/or positions of surface-expressed carbohydrates can evolve to create a continuously changing glycan shield on the surface of the Env protein (Wei *et al.*, 2003). Large sequence variation in the variable loops, including large insertions and deletions, and changes in the number of PNGS in these regions have also been associated with evasion of NAbs (Sagar *et al.*, 2006; Saunders *et al.*, 2005). An especially strong influence of a mutation in the V1/V2 domain on neutralization activity has been reported by a number of investigators (Krachmarov *et al.*, 2005; Pinter *et al.*, 2005; Shibata *et al.*, 2007). However, insertion of a PNGS in the V2 region of the R5 virus during *in vitro* selection using an anti-V3 mAb has not previously been reported.

In this study, we obtained neutralization evading mutants using HIV-1_{BaL} by *in vitro* selection with the anti-V3 mAb, KD-247, and analysed the functional role of the mutations *in vitro*. In the presence of low concentrations of KD-247, viruses with 3 aa mutations in C2 (T240S and I283T) and V3 (T319A) expanded from pre-existing variants in the baseline population. In the presence of high concentrations of KD-247, an increase in the number of mutants that had a PNGS in the V2 region and containing C2 (T240S) and V3 (R315K and F317L) mutations was observed. To identify how each of these mutations affects resistance to KD-247 and the replication kinetics of the virus, we constructed pseudoviruses and infectious clones containing each mutation and combinations of these mutations and compared the IC_{50} and replication kinetics with the wild-type virus. Our results showed that the HIV-1_{BaL} variant with the PNGS in the V2 region and no V3 mutations was sensitive to KD-247. The clone with both the V2 PNGS and mutations in V3 had a high level of resistance to KD-247 and was more resistant than variants with the V3 mutation alone (Table 2). In replication kinetic analyses, the F317L mutation in V3 and the T240S mutation in C2 played a compensatory role for a fitness-loss caused by the V2 PNGS-insertion and R315K mutation in the V3-tip. Our data indicate that the virus with fitness-loss mutations can replicate as well as the wild-type virus to acquire some key mutations in the V3 stem and the C2 region of gp120 with or without exposure to KD-247.

In order to estimate the mechanism of neutralization resistance conferred by the T319A mutation observed at passage 5, we simulated structures of the V3 region using Swiss-PdbViewer software (Supplementary Fig. S1, available in JGV Online) (Guex *et al.*, 1999). According to the simulation data the side chain of arginine at position 315 on the V3 loop in the 315R, 317F and 319A variant at passage 5 was bent to the C-terminal side of the protein compared with its position in the 315R, 317F and 319T variant. It is possible that alanine at position 319 may contribute to KD-247 resistance by altering the three dimensional conformation of the V3 loop.

Our initial analysis using pseudoviruses suggested that the variant with the PNGS alone was sensitive to KD-247

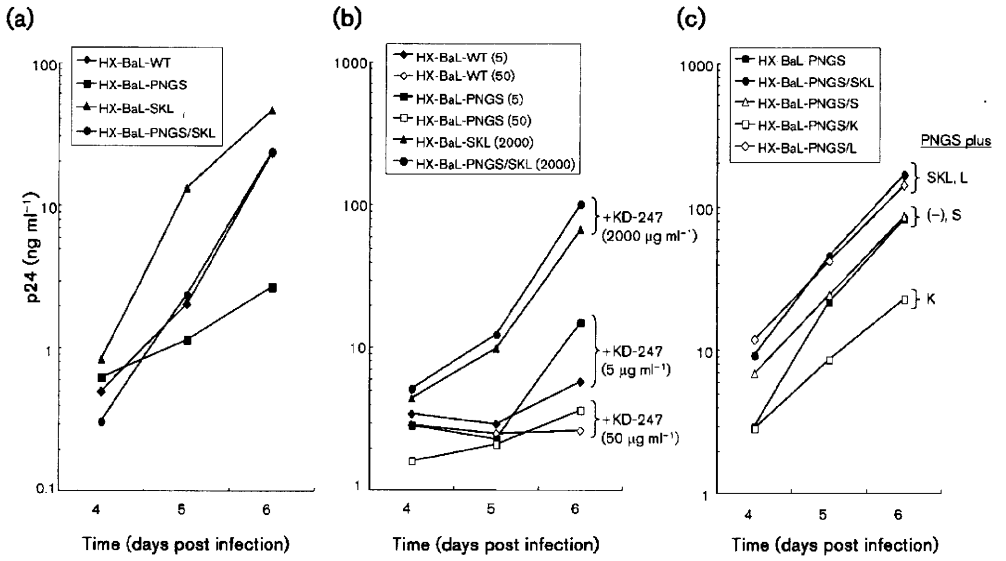

Fig. 5. Viral infectivity of HIV-1 infectious clones with recombinant HIV-1_{BaL} mutant env genes. HIV-1 infectious clones with the env gene sequences listed in Fig. 3 were prepared as described in Methods. PM1/CCR5 cells were exposed to the infectious clones [input p24 amount; (a) 2 ng and (b, c) 10 ng] and cultured for 6 days in the presence or absence of KD-247. The replication of the infectious clones with mutant Env was monitored by measuring the amounts of p24 Gag protein produced in the culture supernatants in the absence (a) or presence (b) of KD-247. The clones with a PNGS and various other mutations were also monitored in the absence of KD-247 (c).

(Fig. 4a). Moreover, the difference in neutralization sensitivity between the viruses with the V3 mutations alone or those with the V2 modifications was not clear in this single round assay (Fig. 4a). We then constructed a panel of replication competent viruses to compare resistance. As shown in Table 2 HX-BaL-PNGS/K containing the R315K mutation in V3 and the PNGS demonstrated a high level of resistance to KD-247 when compared with HX-BaL-K containing the R315K mutation alone. These data suggest that the contribution of the PNGS in neutralization resistance was moderate in a single cycle of viral replication but played a significant role in multiple rounds of infection. It is also possible that the existence of the other mutations such as T240S and F317L in the pseudovirus might have some influence on neutralization sensitivity.

Table 2. Anti-HIV-1 activities of KD-247 and the CCR5 inhibitor, maraviroc

Mutant virus	$IC_{50} \pm$ SD of maraviroc (nM)*	$IC_{50} \pm$ SD of KD-247 (μg ml^{-1})*
HX-BaL-WT	2.0±0.72	0.092±0.028
HX-BaL-PNGS	1.2±0.28	0.047±0.028
HX-BaL-Q	1.9±1.3	0.12±0.047
HX-BaL-S	1.8±0.72	0.087±0.021
HX-BaL-L	2.6±0.33	0.036±0.012
HX-BaL-STA	2.5±1.7	4.6±0.71
HX-BaL-PNGS/SKL	2.4±0.29	214±84
HX-BaL-K	1.6±0.35	285±76†‡‖
HX-BaL-PNGS/K	2.7±0.52	582±59†‡§
HX-BaL-Q/K	1.6±0.32	276±31†§‖

*TZM-bl cells (2×10^4 cells per well) were exposed to 300 $TCID_{50}$ of the infectious clones with wild-type or mutant Env in the presence of various concentrations of maraviroc or KD-247, and incubated for 48 h. IC_{50} values were determined by using a chemiluminescent assay for β-galactosidase detection. All assays were conducted in duplicate or triplicate and the data shown represent means ± SD from the results of three independent experiments.

†*P*-values <0.05 were considered statistically significant (Student's *t*-test). ‡*P*=0.006, §*P*=0.007, ‖*P*=0.89.

Although we did not examine whether the PNGS in V2 at position 186 was actually glycosylated or not, previous studies describing the assignment of glycosylation sites for IIIB and SF2 gp120 show that it is glycosylated (Cutalo *et al.*, 2004; Zhu *et al.*, 2000). The difference in neutralization resistance of HX-BaL-PNGS/K which has the PNGS-insertion in V2 with the counterpart HX-BaL-Q/K of amino acid insertion without glycosylation further supports glycosylation of the site in HIV-1_{BaL} Env (Table 2). HX-BaL-PNGS, which contained the PNGS alone, demonstrated low levels of p24 production compared with the wild-type (Fig. 5a). Moreover, the variant with the R315K mutation in addition to the PNGS further hindered the replication capacity of the variant (Fig. 5c). Interestingly, HX-PNGS-SKL, which contained the additional T240S mutation in the C2 and F317L in the V3 regions, could replicate at the same level as the wild-type clone. These

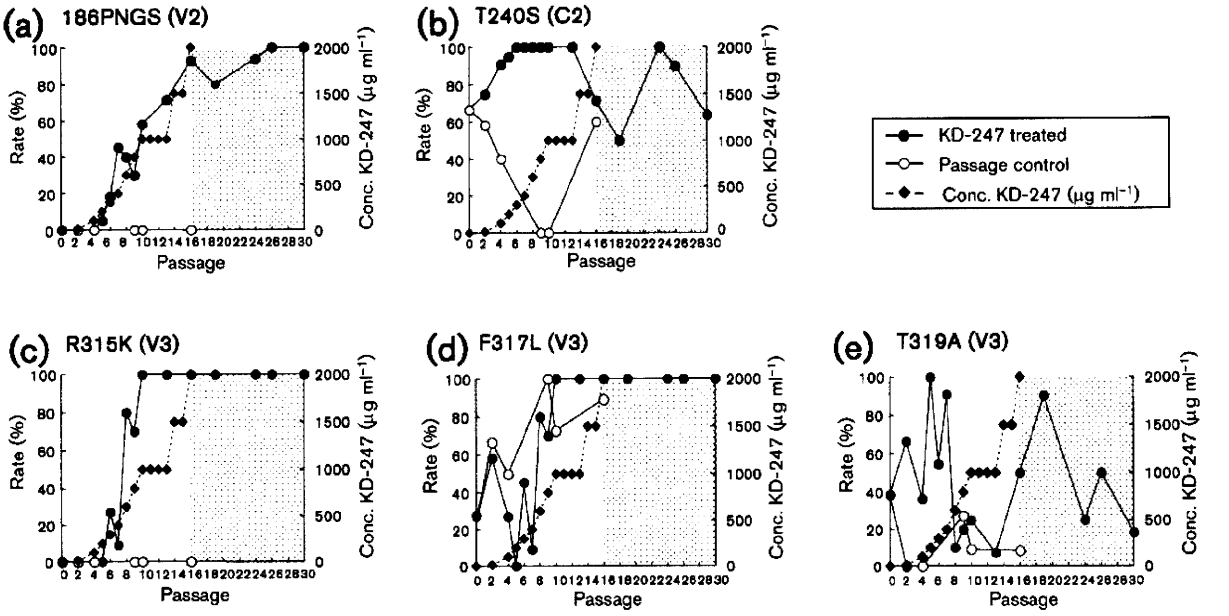

Fig. 6. The gp120 mutation profile of KD-247 HIV-1_{BaL} evasion variants for 14 additional passages without KD-247. The ratio of the PNGS insertion in the V2 region and mutations in the C2 and V3 region of HIV-1_{BaL} evasion variants in gp120 were plotted for 16 passages in the presence of KD-247 and an additional 14 passages in the absence of the mAb. The *y*-axis shows the percentage of PNGS insertions or mutations in the tested clones. The *x*-axis shows the concentration of KD-247.

observations indicate the role of the PNGS and the V3 mutation in neutralization resistance, together with the contribution of two other mutations which compensate for loss in replication ability induced by the first mutations in the process of neutralization evasion.

The interaction of V1/V2 with V3, including the influence on V2 glycosylation, has been reported not only for the neutralization sensitivity but also coreceptor usage (Bontjer *et al.*, 2009; Nabatov *et al.*, 2004). Additionally, mutations associated with resistance to CCR5 antagonists have been mapped to the V3 loop of gp120 and in some cases, to the outside of V3 including the N terminus of gp41 (Anastassopoulou *et al.*, 2009; Baba *et al.*, 2007; Berro *et al.*, 2009; Kuhmann *et al.*, 2004; Marozsan *et al.*, 2005; Ogert *et al.*, 2008; Westby *et al.*, 2007). We then evaluated pseudoviruses and infectious clones derived from the evasion mutants for their sensitivities to maraviroc and a mAb to CCR5 (2D7). As shown in Fig. 4(c, d) and Table 2, no change in co-receptor usage or sensitivity to maraviroc was observed in the evasion mutants.

To elucidate the stability of these evasion variants, we cultured HIV-1_{BaL} (2000) p16 viruses in the absence of KD-247 (Fig. 6). Despite culturing these viruses for 14 passages, no decrease in the proportion of the population containing the PNGS or the R315K, T240S and F317L mutations was observed. The T319A mutation appeared to subside at passage 30. Bunnik *et al.* (2008) reported that reversion of NAb-induced changes in amino acid usage in Env was observed at a late stage of infection in the face of declining neutralizing immunity, suggesting a negative effect of these changes on viral fitness (Bunnik *et al.*, 2008). In contrast, our results suggest that the addition of compensatory amino acid changes can stabilize the replication capacity of the evasion variants with the PNGS and R315K mutation.

In conclusion, we induced highly resistant viral variants against anti-V3 mAb, KD-247, harbouring a PNGS in the V2 region and a V3 mutation, together with mutations that compensate for replication deficiencies induced by the resistant mutations. The mutations associated with viral evasion may play a role in multiple different mechanisms which contribute towards evasion of antibody neutralization. The elucidation of the interplay between these mutations which results in neutralization evasion of the virus has important implications for the development of effective vaccines against HIV-1.

METHODS

Cells, culture conditions, reagents and viruses. PM1/CCR5 cells (Yusa *et al.*, 2005) were maintained in RPMI 1640 medium (Sigma) supplemented with 10% heat-inactivated fetal calf serum (FCS; HyClone), 50 U penicillin ml^{-1}, 50 mg streptomycin ml^{-1} and 100 μg G418 (Nacalai) ml^{-1}. TZM-bl cells (Platt *et al.*, 1998; Wei *et al.*, 2002) obtained from the AIDS Research and Reference Reagent Program (ARRRP) and 293T cells were maintained in Dulbecco's modified Eagle's medium (DMEM; Sigma) supplemented with 10% FCS. KD-247 was provided by the Chemo-Sero-Therapeutic Research

Institute (Eda *et al.*, 2006). The mAb, 2D7, was purchased from BD Biosciences Pharmingen. Human recombinant soluble CD4 (rsCD4) was purchased from R&D Systems. Maraviroc, a CCR5 inhibitor, was a gift from Pfizer Inc. The R5 isolate, HIV-1_{BaL} (Gartner *et al.*, 1986), was passaged in PM1/CCR5 cells and the culture supernatant was stored at −150 °C prior to use.

Isolation of a KD-247-resistant mutant from HIV-1_{BaL} *in vitro*. The selection of KD-247 evasion variants from HIV-1_{BaL} was performed as described previously (Yoshimura *et al.*, 2006). Briefly, PM1/CCR5 cells (4×10^4) were exposed to 500 times $TCID_{50}$ of HIV-1_{BaL} pre-incubated with KD-247 for 30 min at 37 °C. After incubation for 5 h, cells were centrifuged, resuspended in RPMI 1640 medium supplemented with 10 % FCS without KD-247. The culture supernatant was harvested on day 6 and used to infect fresh PM1/CCR5 cells for the next round of culture in the presence of increasing concentrations of KD-247. When the virus began to propagate rapidly in the presence of KD-247, the mAb concentration was further increased. After the virus had been passaged in the presence of up to 2000 μg KD-247 ml^{-1}, the KD-247-resistant virus, HIV-1_{BaL} (2000) p16, was recovered from the cell culture supernatant. After 16 passages with KD-247, we continued culturing the virus for a further 14 passages without KD-247. HIV-1_{BaL} virus was also passaged for the same period in PM1/CCR5 cells in the absence of KD-247, and the resulting virus was designated HIV-1_{BaL} (−) p16. Proviral DNA (pDNA) from infected cells at various passages was subjected to DNA sequencing.

Amplification of pDNA and nucleotide sequencing. pDNA was extracted and nested PCR was performed to amplify the gp120 C1–C4 coding region as described previously (Wang *et al.*, 2002). The primers used were as follows: for the first-step PCR, 1B (5′-AGAAAGAGCAGAAGACAGTGGCAATGA-3′) and H (5′-TAGTGCTTCCTGCTGCTCCCAAGAACCC-3′); for the second-step PCR, 2B (5′-AGCAGAAGACAGTGGCAATGAGAGTGA-3′) and F (5′-ATATAATTCACTTCTCCAATTGTCCCTCAT-3′). The PCR products were inserted into a TA vector (Invitrogen) and sequenced.

Neutralization-sensitivity assay. The neutralization-sensitivity of each passaged HIV-1_{BaL} virus to KD-247 was determined by using TZM-bl cells. Briefly, a virus concentration of 300 $TCID_{50}$ was incubated with various dilutions of KD-247 in duplicate for 30 min at 37 °C in a 96-well flat-bottom culture plate (Corning-Costar). Freshly trypsinized cells (2×10^4 cells in 50 μl of 10 % FCS/DMEM containing 10 μg DEAE-dextran ml^{-1}) were added to each well. After incubation for 2 days at 37 °C, β-galactosidase activity in each well was measured by using Galacto-Star substrate (Applied Biosystems).

Construction of mutant envelope expression vectors. pDNA isolated from the infected cells at various passages was cloned into envelope expression vectors as described previously (Li *et al.*, 2005; Shibata *et al.*, 2007). Briefly, we amplified the full-length gp160 regions from the most frequent clones at the baseline, passage 5 and passage 13 by using LA *Taq* (Takara) with primers ENVA (5′-GGCTTAGGCATCTCCTATGGCAGGAAGAA-3′) and ENVN (5′-CTGCCAATCAGGGAAGTAGCCTTGTGT-3′), and the PCR products were inserted into the pCR-XL-TOPO vector (Invitrogen) and designated pCR-XL-BaL-WT, pCR-XL-BaL-p5 and pCR-XL-BaL-p13, respectively. Chimeric vectors were generated based on the pCR-XL-BaL-WT by replacing the fragments from pCR-XL-BaL-p5 and pCR-XL-BaL-p13 digested at the restriction enzyme sites indicated below. The *NdeI–ScaI* fragment for the pCR-XL-BaL-p5 env gene was subcloned into pCR-XL-BaL-WT, designated pCR-XL-BaL-STA. The *NdeI–ScaI*, *NdeI–StuI* and *StuI–ScaI* fragments for the pCR-XL-BaL-p13 env gene were subcloned into the pCR-XL-BaL-WT, designated pCR-XL-BaL-PNGS/SKL, pCR-XL-BaL-PNGS and pCR-XL-BaL-SKL, respectively. Each *Eco*RI fragment of these vectors was ligated into pCXN2 to give pCXN-BaL-WT, pCXN-BaL-STA, pCXN-BaL-PNGS/SKL, pCXN-BaL-PNGS and pCXN-BaL-SKL.

Pseudovirus preparation. Approximately 5 μg pSG3$^{\Delta env}$ (Wei *et al.*, 2002) and 0.5 μg pRSV-Rev (Hope *et al.*, 1990), supplied by the ARRRP and 4.5 μg HIV-1_{BaL} env-expressing $pCXN_2$ were co-transfected into 293T cells. At 24 h after transfection, the pseudovirus-containing supernatants were harvested, filtered and stored at −150 °C.

A single-round assay for measuring neutralization of the pseudoviruses. A single-round infectivity assay was used to measure the neutralization of HIV-1_{BaL} pseudoviruses as described previously (Li *et al.*, 2005). Briefly, reagents including an entry inhibitor, mAbs or rsCD4 at various concentrations and a pseudovirus suspension corresponding to 300 $TCID_{50}$ were pre-incubated for 30 min at 37 °C. The virus-compound mixtures were added to TZM-bl cells in a 96-well plate (2×10^4 cells per well). After incubation for 2 days at 37 °C, the β-galactosidase activity in each well was measured as described above. The reduction in infectivity was determined by comparing the relative light units in the presence and absence of each compound and was expressed as the percentage of neutralization.

Construction of chimeric pWT10/BaL env proviruses. Chimeric proviruses were constructed from the pWT/BaL proviral plasmid (from the ARRRP) (Hwang *et al.*, 1991) by replacing the region encoding the envelope gp160. Briefly, the env genes obtained from escaped HIV-1_{BaL} variants or induced by site-directed mutagenesis were substituted into the pWT/BaL vectors after digestion at the restriction enzyme sites *SalI* and *Bam*HI. The resulting replication-competent viruses were designated HX-BaL-X (e.g. HX-BaL-WT, HX-BaL-PNGS/SKL etc.).

Preparation of infectious clones and viral replication assays in PM1/CCR5 cells. Approximately, 5 μg of the plasmids from the env mutants were transfected into 293T cells by using the Effectene transfection reagent (Qiagen). At 48 h after transfection, the virus-containing supernatants were harvested, filtered and frozen in aliquots at −150 °C. Viral yields were quantified by using the HIV-1 p24 antigen ELISA (ZeptoMetrix). PM1/CCR5 cells (3×10^4) were exposed to pWT/BaL env chimeric viruses corresponding to 2 ng or 10 ng of p24 for 4 h at 37 °C. Following incubation, cells were centrifuged and resuspended in RPMI 1640 medium supplemented with 10 % FCS and cultured for 6 days. Viral replication was monitored by measuring the concentration of p24 antigen in culture supernatants.

Statistical analysis. Statistical correlations were analysed by using the Student's *t*-test. *P*-values <0.05 were considered statistically significant.

Nucleotide sequence accession numbers. The sequence data of env expression vectors from passaged samples have been deposited under the GenBank accession numbers AB521136–AB521148.

ACKNOWLEDGEMENTS

We thank the Chemo-Sero-Therapeutic Research Institute for kindly providing us with KD-247. The following reagents were obtained through the ARRRP: TZM-bl and pSG3$^{\Delta env}$ from Dr Kappes and Dr Wu; pWT/BaL from Dr Cullen. This work was supported in part by the Program of Founding Research Centres for Emerging and Re-emerging Infectious Diseases and by the Global COE program Global Education and Research Center Aiming at the Control of AIDS and by a grant-in-aid for scientific research (C-21591295) supported by the Ministry of Education, Science, Sports and Culture, Japan; and

a grant from the Ministry of Health, Welfare and Labour of Japan (H21-AIDS-010).

REFERENCES

Anastassopoulou, C. G., Ketas, T. J., Klasse, P. J. & Moore, J. P. (2009). Resistance to CCR5 inhibitors caused by sequence changes in the fusion peptide of HIV-1 gp41. *Proc Natl Acad Sci U S A* **106**, 5318–5323.

Baba, M., Miyake, H., Wang, X., Okamoto, M. & Takashima, K. (2007). Isolation and characterization of human immunodeficiency virus type 1 resistant to the small-molecule CCR5 antagonist TAK-652. *Antimicrob Agents Chemother* **51**, 707–715.

Berro, R., Sanders, R. W., Lu, M., Klasse, P. J. & Moore, J. P. (2009). Two HIV-1 variants resistant to small molecule CCR5 inhibitors differ in how they use CCR5 for entry. *PLoS Pathog* **5**, e1000548.

Bontjer, I., Land, A., Eggink, D., Verkade, E., Tuin, K., Baldwin, C., Pollakis, G., Paxton, W. A., Braakman, I. & other authors (2009). Optimization of human immunodeficiency virus type 1 envelope glycoproteins with V1/V2 deleted, using virus evolution. *J Virol* **83**, 368–383.

Bunnik, E. M., Pisas, L., van Nuenen, A. C. & Schuitemaker, H. (2008). Autologous neutralizing humoral immunity and evolution of the viral envelope in the course of subtype B human immunodeficiency virus type 1 infection. *J Virol* **82**, 7932–7941.

Cao, Y., Qin, L., Zhang, L., Safrit, J. & Ho, D. D. (1995). Virologic and immunologic characterization of long-term survivors of human immunodeficiency virus type 1 infection. *N Engl J Med* **332**, 201–208.

Cutalo, J. M., Deterding, L. J. & Tomer, K. B. (2004). Characterization of glycopeptides from HIV-I(SF2) gp120 by liquid chromatography mass spectrometry. *J Am Soc Mass Spectrom* **15**, 1545–1555.

Deeks, S. G., Schweighardt, B., Wrin, T., Galovich, J., Hoh, R., Sinclair, E., Hunt, P., McCune, J. M., Martin, J. N. & other authors (2006). Neutralizing antibody responses against autologous and heterologous viruses in acute versus chronic human immunodeficiency virus (HIV) infection: evidence for a constraint on the ability of HIV to completely evade neutralizing antibody responses. *J Virol* **80**, 6155–6164.

Eda, Y., Takizawa, M., Murakami, T., Maeda, H., Kimachi, K., Yonemura, H., Koyanagi, S., Shiosaki, K., Higuchi, H. & other authors (2006). Sequential immunization with V3 peptides from primary human immunodeficiency virus type 1 produces cross-neutralizing antibodies against primary isolates with a matching narrow-neutralization sequence motif. *J Virol* **80**, 5552–5562.

Frost, S. D., Wrin, T., Smith, D. M., Kosakovsky Pond, S. L., Liu, Y., Paxinos, E., Chappey, C., Galovich, J., Beauchaine, J. & other authors (2005). Neutralizing antibody responses drive the evolution of human immunodeficiency virus type 1 envelope during recent HIV infection. *Proc Natl Acad Sci U S A* **102**, 18514–18519.

Gartner, S., Markovits, P., Markovitz, D. M., Kaplan, M. H., Gallo, R. C. & Popovic, M. (1986). The role of mononuclear phagocytes in HTLV-III/LAV infection. *Science* **233**, 215–219.

Gorny, M. K., Revesz, K., Williams, C., Volsky, B., Louder, M. K., Anyangwe, C. A., Krachmarov, C., Kayman, S. C., Pinter, A. & other authors (2004). The V3 loop is accessible on the surface of most human immunodeficiency virus type 1 primary isolates and serves as a neutralization epitope. *J Virol* **78**, 2394–2404.

Guex, N., Diemand, A. & Peitsch, M. C. (1999). Protein modelling for all. *Trends Biochem Sci* **24**, 364–367.

Hope, T. J., Huang, X. J., McDonald, D. & Parslow, T. G. (1990). Steroid-receptor fusion of the human immunodeficiency virus type 1 Rev transactivator: mapping cryptic functions of the arginine-rich motif. *Proc Natl Acad Sci U S A* **87**, 7787–7791.

Hwang, S. S., Boyle, T. J., Lyerly, H. K. & Cullen, B. R. (1991). Identification of the envelope V3 loop as the primary determinant of cell tropism in HIV-1. *Science* **253**, 71–74.

Johnson, W. E. & Desrosiers, R. C. (2002). Viral persistence: HIV's strategies of immune system evasion. *Annu Rev Med* **53**, 499–518.

Joos, B., Trkola, A., Kuster, H., Aceto, L., Fischer, M., Stiegler, G., Armbruster, C., Vcelar, B., Katinger, H. & Gunthard, H. F. (2006). Long-term multiple-dose pharmacokinetics of human monoclonal antibodies (MAbs) against human immunodeficiency virus type 1 envelope gp120 (MAb 2G12) and gp41 (MAbs 4E10 and 2F5). *Antimicrob Agents Chemother* **50**, 1773–1779.

Krachmarov, C., Pinter, A., Honnen, W. J., Gorny, M. K., Nyambi, P. N., Zolla-Pazner, S. & Kayman, S. C. (2005). Antibodies that are cross-reactive for human immunodeficiency virus type 1 clade A and clade B V3 domains are common in patient sera from Cameroon, but their neutralization activity is usually restricted by epitope masking. *J Virol* **79**, 780–790.

Kuhmann, S. E., Pugach, P., Kunstman, K. J., Taylor, J., Stanfield, R. L., Snyder, A., Strizki, J. M., Riley, J., Baroudy, B. M. & other authors (2004). Genetic and phenotypic analyses of human immunodeficiency virus type 1 escape from a small-molecule CCR5 inhibitor. *J Virol* **78**, 2790–2807.

Kwong, P. D., Doyle, M. L., Casper, D. J., Cicala, C., Leavitt, S. A., Majeed, S., Steenbeke, T. D., Venturi, M., Chaiken, I. & other authors (2002). HIV-1 evades antibody-mediated neutralization through conformational masking of receptor-binding sites. *Nature* **420**, 678–682.

Li, M., Gao, F., Mascola, J. R., Stamatatos, L., Polonis, V. R., Koutsoukos, M., Voss, G., Goepfert, P., Gilbert, P. & other authors (2005). Human immunodeficiency virus type 1 env clones from acute and early subtype B infections for standardized assessments of vaccine-elicited neutralizing antibodies. *J Virol* **79**, 10108–10125.

Mahalanabis, M., Jayaraman, P., Miura, T., Pereyra, F., Chester, E. M., Richardson, B., Walker, B. & Haigwood, N. L. (2009). Continuous viral escape and selection by autologous neutralizing antibodies in drug-naive human immunodeficiency virus controllers. *J Virol* **83**, 662–672.

Manrique, A., Rusert, P., Joos, B., Fischer, M., Kuster, H., Leemann, C., Niederost, B., Weber, R., Stiegler, G. & other authors (2007). In vivo and in vitro escape from neutralizing antibodies 2G12, 2F5, and 4E10. *J Virol* **81**, 8793–8808.

Marozsan, A. J., Kuhmann, S. E., Morgan, T., Herrera, C., Rivera-Troche, E., Xu, S., Baroudy, B. M., Strizki, J. & Moore, J. P. (2005). Generation and properties of a human immunodeficiency virus type 1 isolate resistant to the small molecule CCR5 inhibitor, SCH-417690 (SCH-D). *Virology* **338**, 182–199.

Masuda, T., Matsushita, S., Kuroda, M. J., Kannagi, M., Takatsuki, K. & Harada, S. (1990). Generation of neutralization-resistant HIV-1 in vitro due to amino acid interchanges of third hypervariable env region. *J Immunol* **145**, 3240–3246.

McCaffrey, R. A., Saunders, C., Hensel, M. & Stamatatos, L. (2004). N-linked glycosylation of the V3 loop and the immunologically silent face of gp120 protects human immunodeficiency virus type 1 SF162 from neutralization by anti-gp120 and anti-gp41 antibodies. *J Virol* **78**, 3279–3295.

Montefiori, D. C., Hill, T. S., Vo, H. T., Walker, B. D. & Rosenberg, E. S. (2001). Neutralizing antibodies associated with viremia control in a subset of individuals after treatment of acute human immunodeficiency virus type 1 infection. *J Virol* **75**, 10200–10207.

Moore, J. P., Cao, Y., Qing, L., Sattentau, Q. J., Pyati, J., Koduri, R., Robinson, J., Barbas, C. F., III, Burton, D. R. & Ho, D. D. (1995). Primary isolates of human immunodeficiency virus type 1 are relatively resistant to neutralization by monoclonal antibodies to gp120, and their neutralization is not predicted by studies with monomeric gp120. *J Virol* **69**, 101–109.

Nabatov, A. A., Pollakis, G., Linnemann, T., Kliphius, A., Chalaby, M. I. & Paxton, W. A. (2004). Intrapatient alterations in the human immunodeficiency virus type 1 gp120 V1V2 and V3 regions differentially modulate coreceptor usage, virus inhibition by CC/CXC chemokines, soluble CD4, and the b12 and 2G12 monoclonal antibodies. *J Virol* **78**, 524–530.

Ogert, R. A., Wojcik, L., Buontempo, C., Ba, L., Buontempo, P., Ralston, R., Strizki, J. & Howe, J. A. (2008). Mapping resistance to the CCR5 co-receptor antagonist vicriviroc using heterologous chimeric HIV-1 envelope genes reveals key determinants in the C2–V5 domain of gp120. *Virology* **373**, 387–399.

Park, E. J., Vujcic, L. K., Anand, R., Theodore, T. S. & Quinnan, G. V., Jr (1998). Mutations in both gp120 and gp41 are responsible for the broad neutralization resistance of variant human immunodeficiency virus type 1 MN to antibodies directed at V3 and non-V3 epitopes. *J Virol* **72**, 7099–7107.

Pinter, A., Honnen, W. J., He, Y., Gorny, M. K., Zolla-Pazner, S. & Kayman, S. C. (2004). The V1/V2 domain of gp120 is a global regulator of the sensitivity of primary human immunodeficiency virus type 1 isolates to neutralization by antibodies commonly induced upon infection. *J Virol* **78**, 5205–5215.

Pinter, A., Honnen, W. J., D'Agostino, P., Gorny, M. K., Zolla-Pazner, S. & Kayman, S. C. (2005). The C108g epitope in the V2 domain of gp120 functions as a potent neutralization target when introduced into envelope proteins derived from human immunodeficiency virus type 1 primary isolates. *J Virol* **79**, 6909–6917.

Platt, E. J., Wehrly, K., Kuhmann, S. E., Chesebro, B. & Kabat, D. (1998). Effects of CCR5 and CD4 cell surface concentrations on infections by macrophagetropic isolates of human immunodeficiency virus type 1. *J Virol* **72**, 2855–2864.

Pugach, P., Kuhmann, S. E., Taylor, J., Marozsan, A. J., Snyder, A., Ketas, T., Wolinsky, S. M., Korber, B. T. & Moore, J. P. (2004). The prolonged culture of human immunodeficiency virus type 1 in primary lymphocytes increases its sensitivity to neutralization by soluble CD4. *Virology* **321**, 8–22.

Richman, D. D., Wrin, T., Little, S. J. & Petropoulos, C. J. (2003). Rapid evolution of the neutralizing antibody response to HIV type 1 infection. *Proc Natl Acad Sci U S A* **100**, 4144–4149.

Sagar, M., Wu, X., Lee, S. & Overbaugh, J. (2006). Human immunodeficiency virus type 1 V1–V2 envelope loop sequences expand and add glycosylation sites over the course of infection, and these modifications affect antibody neutralization sensitivity. *J Virol* **80**, 9586–9598.

Saunders, C. J., McCaffrey, R. A., Zharkikh, I., Kraft, Z., Malenbaum, S. E., Burke, B., Cheng-Mayer, C. & Stamatatos, L. (2005). The V1, V2, and V3 regions of the human immunodeficiency virus type 1 envelope differentially affect the viral phenotype in an isolate-dependent manner. *J Virol* **79**, 9069–9080.

Shibata, J., Yoshimura, K., Honda, A., Koito, A., Murakami, T. & Matsushita, S. (2007). Impact of V2 mutations on escape from a potent neutralizing anti-V3 monoclonal antibody during in vitro selection of a primary human immunodeficiency virus type 1 isolate. *J Virol* **81**, 3757–3768.

Sullivan, N., Thali, M., Furman, C., Ho, D. D. & Sodroski, J. (1993). Effect of amino acid changes in the V1/V2 region of the human immunodeficiency virus type 1 gp120 glycoprotein on subunit association, syncytium formation, and recognition by a neutralizing antibody. *J Virol* **67**, 3674–3679.

Trkola, A., Kuster, H., Rusert, P., Joos, B., Fischer, M., Leemann, C., Manrique, A., Huber, M., Rehr, M. & other authors (2005). Delay of HIV-1 rebound after cessation of antiretroviral therapy through passive transfer of human neutralizing antibodies. *Nat Med* **11**, 615–622.

Trkola, A., Kuster, H., Rusert, P., von Wyl, V., Leemann, C., Weber, R., Stiegler, G., Katinger, H., Joos, B. & Gunthard, H. F. (2008). In vivo efficacy of human immunodeficiency virus neutralizing antibodies: estimates for protective titers. *J Virol* **82**, 1591–1599.

Wang, F. X., Kimura, T., Nishihara, K., Yoshimura, K., Koito, A. & Matsushita, S. (2002). Emergence of autologous neutralization-resistant variants from preexisting human immunodeficiency virus (HIV) quasi species during virus rebound in HIV type 1-infected patients undergoing highly active antiretroviral therapy. *J Infect Dis* **185**, 608–617.

Wei, X., Decker, J. M., Liu, H., Zhang, Z., Arani, R. B., Kilby, J. M., Saag, M. S., Wu, X., Shaw, G. M. & Kappes, J. C. (2002). Emergence of resistant human immunodeficiency virus type 1 in patients receiving fusion inhibitor (T-20) monotherapy. *Antimicrob Agents Chemother* **46**, 1896–1905.

Wei, X., Decker, J. M., Wang, S., Hui, H., Kappes, J. C., Wu, X., Salazar-Gonzalez, J. F., Salazar, M. G., Kilby, J. M. & other authors (2003). Antibody neutralization and escape by HIV-1. *Nature* **422**, 307–312.

Westby, M., Smith-Burchnell, C., Mori, J., Lewis, M., Mosley, M., Stockdale, M., Dorr, P., Ciaramella, G. & Perros, M. (2007). Reduced maximal inhibition in phenotypic susceptibility assays indicates that viral strains resistant to the CCR5 antagonist maraviroc utilize inhibitor-bound receptor for entry. *J Virol* **81**, 2359–2371.

Yoshimura, K., Shibata, J., Kimura, T., Honda, A., Maeda, Y., Koito, A., Murakami, T., Mitsuya, H. & Matsushita, S. (2006). Resistance profile of a neutralizing anti-HIV monoclonal antibody, KD-247, that shows favourable synergism with anti-CCR5 inhibitors. *AIDS* **20**, 2065–2073.

Yusa, K., Maeda, Y., Fujioka, A., Monde, K. & Harada, S. (2005). Isolation of TAK-779-resistant HIV-1 from an R5 HIV-1 GP120 V3 loop library. *J Biol Chem* **280**, 30083–30090.

Zhu, X., Borchers, C., Bienstock, R. J. & Tomer, K. B. (2000). Mass spectrometric characterization of the glycosylation pattern of HIV-gp120 expressed in CHO cells. *Biochemistry* **39**, 11194–11204.

Zolla-Pazner, S. (2004). Identifying epitopes of HIV-1 that induce protective antibodies. *Nat Rev Immunol* **4**, 199–210.

Bioorganic & Medicinal Chemistry Letters 20 (2010) 354–358

Contents lists available at ScienceDirect

Bioorganic & Medicinal Chemistry Letters

journal homepage: www.elsevier.com/locate/bmcl

CD4 mimics targeting the mechanism of HIV entry

Yuko Yamada [a], Chihiro Ochiai [a], Kazuhisa Yoshimura [b], Tomohiro Tanaka [a], Nami Ohashi [a], Tetsuo Narumi [a], Wataru Nomura [a], Shigeyoshi Harada [b], Shuzo Matsushita [b], Hirokazu Tamamura [a,*]

[a] Institute of Biomaterials and Bioengineering, Tokyo Medical and Dental University, Chiyoda-ku, Tokyo 101-0062, Japan
[b] Center for AIDS Research, Kumamoto University, Kumamoto 860-0811, Japan

ARTICLE INFO

Article history:
Received 19 September 2009
Revised 20 October 2009
Accepted 22 October 2009
Available online 4 November 2009

Keywords:
CD4 mimic
HIV entry
Synergistic effect
CXCR4

ABSTRACT

A structure–activity relationship study was conducted of several CD4 mimicking small molecules which block the interaction between HIV-1 gp120 and CD4. These CD4 mimics induce a conformational change in gp120, exposing its co-receptor-binding site. This induces a highly synergistic interaction in the use in combination with a co-receptor CXCR4 antagonist and reveals a pronounced effect on the dynamic supramolecular mechanism of HIV-1 entry.

Recently, remarkable success has attended the clinical treatment of HIV-infected and AIDS patients, with 'highly active antiretroviral therapy (HAART)'. This approach involves a combination of two or three agents from two categories: reverse transcriptase inhibitors and protease inhibitors.[1] In addition, the molecular mechanism involved in HIV-entry and -fusion into host cells has been described in detail.[2] The complex interactions of surface proteins on cellular and viral membranes, which are designated as a dynamic supramolecular mechanism of HIV entry, are reported to be crucial to the viral infection. In a first step, an HIV envelope protein, gp120 interacts with a cell surface protein, CD4, leading to a conformational change in gp120 followed by subsequent binding of gp120 to a co-receptor CCR5[3] or CXCR4.[4] CCR5 and CXCR4 are the major co-receptors for the entry of macrophage-tropic (R5-) and T cell line-tropic (X4-) HIV-1, respectively. The interaction of gp120 with CCR5 or CXCR4 triggers entry of another envelope protein, gp41 to the cell membrane and formation of a gp41 trimer-of-hairpins structure, which causes fusion of HIV/cell-membranes and completes the infection.

Informed by this mechanism, a fusion inhibitor, enfuvirtide (fuzeon, Trimers & Roche)[5] and a CCR5 antagonist, maraviroc (Pfizer)[6] in addition to an integrase inhibitor, raltegravir (Merck)[7] have been used clinically. However, serious problems with chemotherapy still persist, including the emergence of viral strains with multi-drug resistance (MDR), considerable adverse effects and high costs. Consequently, development of novel drugs possessing mechanisms of action different from those of the above inhibitors is currently required. We have previously developed selective CXCR4 antagonists[8] and fusion inhibitors.[9] Furthermore, *N*-(4-Bromophenyl)-*N*′-(2,2,6,6-tetramethylpiperidin-4-yl)-oxalamide (**1**) and *N*-(4-chlorophenyl)-*N*′-(2,2,6,6-tetramethylpiperidin-4-yl)-oxalamide (**2**) were previously found using chemical library screening to inhibit syncytium formation by other researchers.[10] **1** and **2** bind to gp120 with binding affinities of K_d = 2.2 μM and 3.7 μM, respectively, blocking the interaction of gp120 with CD4 in the first step of an HIV-1 entry. Thus, in the present study we focus on the development of CD4 mimics that can block the interaction between gp120 and CD4. We have investigated the effect of CD4 mimics on conformational changes of gp120 and on their use in combination use with a CXCR4 antagonist.

Initially, molecular modeling of compound **2** docked into gp120 was carried out using docking simulations performed by the FlexSIS module of SYBYL 7.1 (Tripos, St. Louis) (Fig. 1).[11] The atomic coordinates of the crystal structure of gp120 with soluble CD4 (sCD4) were retrieved from Protein Data Bank (PDB) (entry 1RZJ) (Fig. 1a) and it was observed that Phe^{43} and Arg^{59} of the CD4 have multiple contacts with Asp^{368}, Glu^{370} and Trp^{427} of gp120, which are all conserved residues. An inspection of the environment of compound **2** docked in gp120 revealed the presence of a large cavity around the *p*-position of the phenyl ring of compound **2**, which could interact with the viral surface protein gp120 (Fig. 1b and c). Several analogs of **2** with substituents on the phenyl ring were therefore synthesized.

All compounds except **12** were synthesized by previously published methods (Scheme 1).[10b,12,13] Aniline derivatives (**3**) were coupled with ethyl oxalyl chloride to yield the corresponding ethyl oxalamates **4**. Saponification of the above oxalamates to the corresponding free acids and the subsequent coupling with 4-ami-

* Corresponding author.
E-mail address: tamamura.mr@tmd.ac.jp (H. Tamamura).

0960-894X/$ - see front matter © 2009 Elsevier Ltd. All rights reserved.
doi:10.1016/j.bmcl.2009.10.098

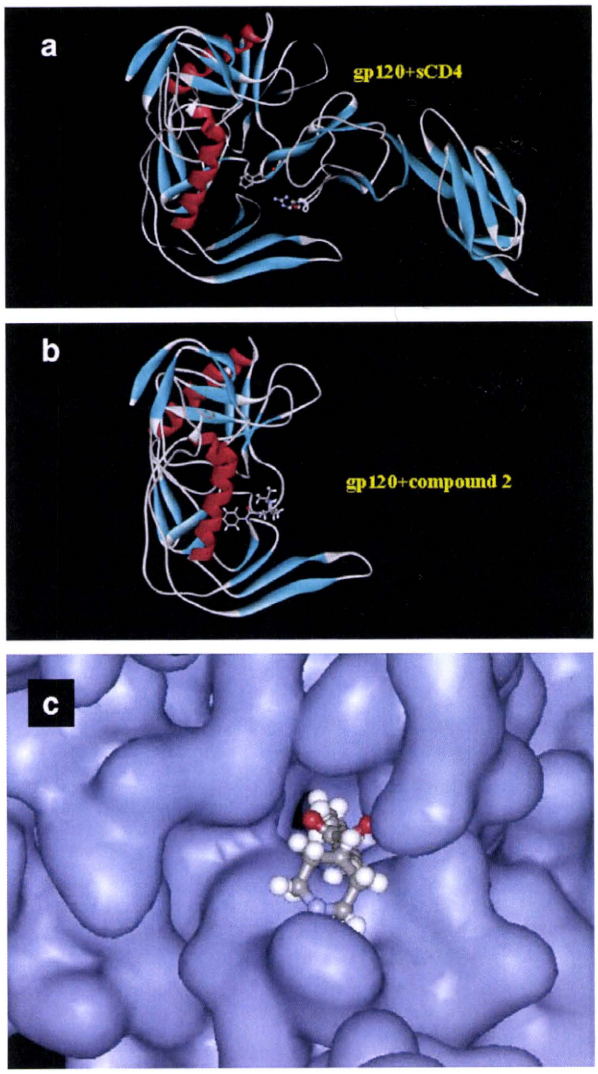

Figure 1. (a) The crystal structure of gp120 with soluble CD4 (sCD4) retrieved from the PDB (entry 1RZJ); (b) docking structure of compound **2** and gp120; (c) a focused figure of (b) shown by space-filling model.

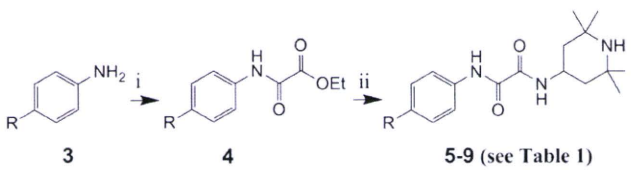

Scheme 1. Reagents and conditions: (i) ethyl oxalyl chloride, Et_3N; (ii) 1 M NaOH; 4-amino-2,2,6,6-tetramethylpiperidine, 1-(3-dimethylaminopropyl)-3-ethylcarbodiimide hydrochloride, 1-hydroxybenzotriazole, Et_3N.

no-2,2,6,6-tetramethylpiperidine using 1-ethyl-3-(3-dimethylaminopropyl)carbodiimide hydrochloride (EDC) and 1-hydroxybenzotriazole (HOBt) yielded compounds **5–9**. In the case of compound **12**, whose amide bond is not stable during the reaction of the saponification of the corresponding oxalamates, an alternative synthetic scheme was used (Scheme 2).[14] The reaction of *p*-nitroaniline (**10**) with oxalyl chloride gave the corresponding oxoacetamide **11**, which was subsequently coupled with 4-amino-2,2,6,6-tetramethylpiperidine to yield the desired compound **12**.

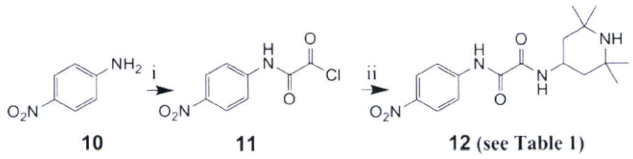

Scheme 2. Reagents and conditions: (i) oxalyl chloride, Et_3N; (ii) 4-amino-2,2,6,6-tetramethylpiperidine, Et_3N.

The anti-HIV activity of the synthetic compounds was evaluated against various viral strains including both laboratory and primary isolates (Table 1). IC_{50} values were determined by the 3-(4,5-dimethylthiazol-2-yl)-2,5-diphenyltetrazolium bromide (MTT) method[15] as the concentrations of the compounds which conferred 50% protection against HIV-1-induced cytopathogenicity in PM1/CCR5 cells. Cytotoxicity of the compounds based on the viability of mock-infected PM1/CCR5 cells was also evaluated using the MTT method. CC_{50} values were determined as the concentrations achieving 50% reduction of the viability of mock-infected cells. Compounds **1** and **2** showed potent anti-HIV activity against laboratory isolates, IIIB (X4, Sub B) and 89.6 (dual, Sub B) strains, and compound **2** also possessed potent activity against a primary isolate, an fTOI strain (R5, Sub B). All of the IC_{50} values were between 4 μM and 10 μM. Compound **1** was not tested against primary isolates. The potencies of compounds **1** and **2** are comparable to the reported binding affinities for gp120 (K_d = 2.2 and 3.7 μM, respectively).[10] Several of the new analogs of compounds **1** and **2** showed significant anti-HIV activity. Compound **5**, which has a phenyl group in place of the *p*-chlorophenyl group of compound **2**, did not show significant anti-HIV activity at concentrations below 100 μM against all strains tested except for an fTOI strain (R5, Sub B). This result suggests that a substituent at the *p*-position of the phenyl ring is critical for potent activity. Compound **6**, which has a fluorine atom at the *p*-position of the phenyl ring, showed moderate anti-HIV activity against laboratory isolates, IIIB (X4, Sub B) and 89.6 (dual, Sub B) strains (IC_{50} = 61 and 81 μM, respectively), but, at concentrations below 100 μM, failed to show significant anti-HIV activity against a primary isolate, a KYAG strain (R5, Sub B). Among halogen atoms, fluorine is less suitable than bromine or chlorine as a substituent at the *p*-position of the phenyl ring, as evidenced by compound **6**, which is 8–15-fold less potent than compounds **1** and **2** against IIIB (X4, Sub B) and 89.6 (dual, Sub B) strains. Compound **7**, which has a methyl group at the *p*-position of the phenyl ring, showed relatively more potent activity against IIIB (X4, Sub B) and 89.6 (dual, Sub B) strains (IC_{50} = 23 and 41 μM, respectively) than compound **6**. Compound **7** also showed significant anti-HIV activity against primary isolates, fTOI (R5, Sub B) and KYAG (R5, Sub B) strains (IC_{50} = 16 and 51 μM, respectively). Compound **8**, with a methoxy group at the *p*-position of the phenyl ring, did not show significant anti-HIV activity against all strains tested until a concentration of 100 μM was reached. In the biological assays, derivatives having electron-withdrawing substituents such as bromine, chlorine and fluorine at the *p*-position of the phenyl ring are relatively potent, whereas derivatives having electron-donating groups such as methoxy at this position are not potent. Furthermore, the steric effect of a substituent at the *p*-position of the phenyl ring appears to be critical to anti-HIV activity. The sum of Hammett constants (σ) of benzoic acid substituents[16] shown in Table 1 can be used to evaluate the electron-withdrawing or -donating effect of the substituents on the aromatic ring. The Taft E_s values[16a,17] were used as steric parameters for substituents at the *p*-position of the phenyl ring. The order of potency found for the halogen-containing derivatives in anti-HIV activity against laboratory isolates, IIIB (X4, Sub B) and 89.6 (dual, Sub B), is: compound **1** (R = Br) (σ = 0.23, E_s = −1.16), **2**

Table 1
Hammett constants (σ) and steric effects (E_s) of substituted aromatic rings and anti-HIV activity and cytotoxicity of synthetic compounds

Compd	R[a]	σ[b]	E_s[c]	IC_{50}[e] (μM)				CC_{50}[e] (μM)
				Lab. isolates		Primary isolates		
				IIIB (X4)	89.6 (dual)	fTOI (R5)	KYAG (R5)	
1	Br	0.23	−1.16	4	9	ND	ND	150
2	Cl	0.23	−0.97	8	10	5	>30	170
5	H	0	0	>100	>100	81	>100	350
6	F	0.06	−0.46	61	81	ND	>100	320
7	CH_3	−0.17	−1.24	23	41	16	51	210
8	OCH_3	−0.27	−0.55	>100	>100	ND	>100	340
9	CF_3	0.54	−2.40	ND	27	ND	ND	72
12	NO_2	0.78	−1.77[d]	ND	42	ND	ND	230
sCD4				0.010	0.021	0.0044	ND	ND

[a] See Schemes 1 and 2.
[b] σ = Hammett constant of a substitutent on a benzoic acid derivative.[16]
[c] E_s = steric effect of a substituent at the *para* position on the aromatic ring.[16a,17]
[d] The average value of −1.01 and −2.52, which are E_s values of the NO_2 group, −1.77, was used.
[e] Values are means of at least three experiments (ND = not determined).

(R = Cl) (σ = 0.23, E_s = −0.97), **6** (R = F) (σ = 0.06, E_s = −0.46) and **5** (R = H) (σ = 0, E_s = 0). This is the order of substituents' electron-withdrawing ability and also of their size. Methyl (σ = −0.17, E_s = −1.24) is an electron-donating group, but is almost as bulky as a bromine atom. Thus, the *p*-methyl derivative **7** has relatively potent anti-HIV activity against laboratory isolates, IIIB (X4, Sub B) and 89.6 (dual, Sub B), higher than that of compound **6** (R = F) but lower than that of compound **1** (R = Br) or **2** (R = Cl). The electron-donating ability of a methoxy group is stronger (σ = −0.27), but the bulk size is smaller (E_s = −0.55), than that of a methyl group. Thus, the *p*-methoxy derivative **8** has no significant anti-HIV activity against all strains tested at concentrations below 100 μM. Two derivatives containing bulkier and more potent electron-withdrawing substituents such as trifluoromethyl (R = CF_3) (σ = 0.54, E_s = −2.40) and nitro (R = NO_2) (σ = 0.78, E_s = −1.77) at the *p*-position of the phenyl ring were evaluated. Compounds **9** (R = CF_3) and **12** (R = NO_2) showed significant anti-HIV activity against an 89.6 (dual, Sub B) strain. These are less potent than compounds **1** and **2** and this is perhaps due to the excessive size of the substituents at the *p*-position. This suggests that a certain level of the bulk size and a potent electron-withdrawing ability of the substituents are preferable for anti-HIV activity. It is estimated that a cavity around the *p*-position of the phenyl ring of CD4 mimicking compounds would be optimally filled by bromine (E_s = −1.16) or a methyl group (E_s = −1.24) at *p*-position, and that an electron-deficient aromatic ring might interact tightly with a negatively charged group such as carboxy of Glu^{370}. In isothermal titration calorimetry (ITC) experiments reported elsewhere,[10c] compound **5** (R = H) does not have significant affinity for gp120, and compound **6** (R = F) has less potent affinity for gp120 than compound **2**, consistent with the present data. In all but one of the compounds, no significant cytotoxicity was detected (CC_{50} >150 μM, Table 1), the exception being compound **9** (R = CF_3) (CC_{50} = 72 μM). Compounds **7** and **12** have relatively low cytotoxicities, compared to compounds **1** and **2**.

Fluorescence activated cell sorting (FACS) analysis was performed[15] to investigate whether these synthetic compounds interact with gp120 inducing the conformational change necessary for the approach of an anti-envelope antibody or a co-receptor to the gp120. The profile of binding of an anti-envelope CD4-induced monoclonal antibody, 4C11, to the Env-expressing cell surface (an R5-HIV-1 strain, JR-FL,-infected PM1 cells) pretreated with the above CD4 mimic analogs was examined. Comparison of the binding of 4C11 to the cell surface was measured in terms of the mean fluorescence intensity (MFI), and is shown in Figure 2. Pretreatment of the Env-expressing cells with compound **2** (MFI = 38.42) produced a remarkable increase in binding affinity for 4C11, similar to that observed in pretreatment with sCD4 (MFI = 37.90). This is consistent with the results in the previous paper[10] where it was reported that compound **2** enhances the binding of gp120 to the 17b monoclonal antibody which recognizes the co-receptor binding site of gp120. Env-expressing cells, which were not pretreated with sCD4 or a CD4 mimic compound, did not show significant binding affinity for 4C11 (Fig. 2, blank). The increase in binding affinity for monoclonal antibodies may be due to conformational changes in gp120, which were caused by the interaction of sCD4 or a CD4 mimic with gp120. It is hypothesized that such conformational changes involve the exposure of the co-receptor binding site of gp120 (the V3 loop), which is hidden internally, since the binding of gp120 to 17b is enhanced. Compound **5**, which failed to show significant anti-HIV activity, and compounds **7**, **9** and **12**, which had significant anti-HIV activity, were assessed in the FACS analysis. The profile of the binding of 4C11 to the Env-expressing cell surface pretreated with compound **5** (MFI = 14.34) was similar to that of the blank (MFI = 11.24), suggesting that compound **5** offers no significant enhancement of binding affinity for 4C11. This result is compatible with the anti-HIV activity of compound **5**. The profile of the binding of 4C11 to the Env-expressing cell surface pretreated with compound **7** (MFI = 38.33) was entirely similar to that of compound **2** used as a pretreatment. Pretreatment of the cell surface with compounds **9** and **12** (MFI = 29.09 and 30.01, respectively) produced a slightly lower enhancement of binding affinity for 4C11, compared to those of compounds **2** and **7** as pretreatments. However, in the ITC experiments reported elsewhere,[10c] compound **9** (R = CF_3) has a high affinity for gp120, comparable to that of compound **2**, but compound **12** (R = NO_2) does not have significant affinity for gp120, indicating that these are not consistent with the current FACS studies, possibly due to the difference in the assay systems. Although the anti-HIV activity of **7** is weaker than that of compound **2**, the level of compound **7** inducing an enhancement of binding affinity of gp120 for 4C11 is comparable to that of compound **2**. The concentration of compounds used in the FACS analysis was 100 μM, much beyond the IC_{50} values of compounds **2** and **7**. A concentration of 100 μM would be also sufficient for the expression of anti-HIV activity caused by compounds **2** and **7**.

An effect on the use of compound **2** combined with another entry inhibitor was investigated. Analysis of the synergistic effects of anti-HIV agents was performed according to the median effect principle using the CalcuSyn version 2 computer program[18] to estimate IC_{50} values of compounds in different combinations. Combination indices (CI) were estimated from the data evaluated using the MTT assay

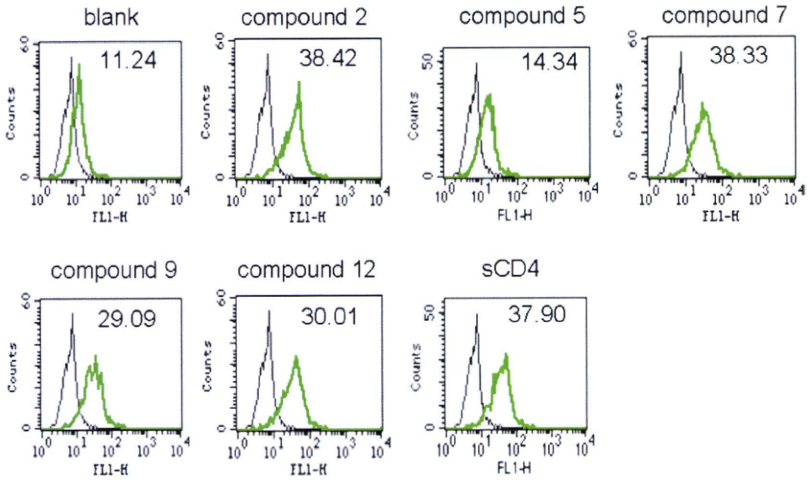

Figure 2. JR-FL (R5, Sub B) chronically infected PM1 cells were preincubated with 100 μM of a CD4 mimic or sCD4 (11 nM) for 15 min, and then incubated with an anti-HIV-1 mAb, 4C11, at 4 °C for 15 min. The cells were washed with PBS, and fluorescein isothiocyanate (FITC)-conjugated goat anti-human IgG antibody was used for antibody-staining. Flow cytometry data for the binding of 4C11 (green lines) to the Env-expressing cell surface in the presence of sCD4 or a CD4 mimic are shown among gated PM1 cells along with a control antibody (anti-human CD19: black lines). Data are representative of the results from a minimum of two independent experiments. The number at the top of each graph shows the mean fluorescence intensity (MFI) of the antibody 4C11.

Table 2
Combination indices (CI) for compound **2** or sCD4 and a CXCR4 antagonist, T140, against an HIV IIIB strain

Combination	HIV strain	CI values at different IC[a]		
		IC_{50}	IC_{75}	IC_{90}
2 + T140	IIIB	0.786	0.713	0.655
sCD4 + T140	IIIB	0.705	0.528	0.400

[a] The multiple-drug effect analysis reported by Chou et al. was used to analyze the effects of combinational uses of compounds.[18] CI <0.9: synergy, 0.9 < CI < 1.1: additivity, CI >1.1: antagonism.

(Table 2).[15] Compound **2** showed a highly remarkable synergistic anti-HIV activity with a co-receptor CXCR4 antagonist, T140,[8a] against an X4-HIV-1 strain, IIIB at various IC values (IC_{50}, IC_{75} and IC_{90}). However, sCD4 exhibited a higher synergistic effect (lower CI values) with T140 (Table 2). The interaction of sCD4 or a CD4 mimic with gp120 would expose the co-receptor-binding site of gp120, and the co-receptor CXCR4 could then easily approach gp120. Thus, an inhibitory effect of a CXCR4 antagonist would be meaningful, and a significant synergistic effect might also be brought about by a combination of sCD4 or a CD4 mimic and T140.

In summary, a series of CD4 mimic compounds were synthesized and evaluated for their anti-HIV activity. Several compounds showed significant anti-HIV activity with relatively low cytotoxicity. SAR studies showed that a certain level of size and electron-withdrawing ability of the substituents at the *p*-position of the phenyl ring are suitable for potent anti-HIV activity. In addition, the treatment of Env-expressing cells with several CD4 mimicking compounds causes a conformational change, exposing the co-receptor-binding site of gp120 externally. Thus, a CD4 mimic exhibited a remarkable synergistic effect with a co-receptor antagonist. These compounds are essential probes directed to the dynamic supramolecular mechanism of HIV entry, and important leads for the cocktail therapy of AIDS.

Acknowledgments

This work was supported by Mitsui Life Social Welfare Foundation, Grant-in-Aid for Scientific Research from the Ministry of Education, Culture, Sports, Science, and Technology of Japan, and Health and Labour Sciences Research Grants from Japanese Ministry of Health, Labor, and Welfare.

References and notes

1. Mitsuya, H.; Erickson, J. In *Textbook of AIDS Medicine*; Merigan, T. C., Bartlett, J. G., Bolognesi, D., Eds.; Williams & Wilkins: Baltimore, 1999; pp 751–780.
2. Chan, D. C.; Kim, P. S. *Cell* **1998**, *93*, 681.
3. (a) Alkhatib, G.; Combadiere, C.; Broder, C. C.; Feng, Y.; Kennedy, P. E.; Murphy, P. M.; Berger, E. A. *Science* **1996**, *272*, 1955; (b) Choe, H.; Farzan, M.; Sun, Y.; Sullivan, N.; Rollins, B.; Ponath, P. D.; Wu, L.; Mackay, C. R.; LaRosa, G.; Newman, W.; Gerard, N.; Gerard, C.; Sodroski, J. *Cell* **1996**, *85*, 1135; (c) Deng, H. K.; Liu, R.; Ellmeier, W.; Choe, S.; Unutmaz, D.; Burkhart, M.; Marzio, P. D.; Marmon, S.; Sutton, R. E.; Hill, C. M.; Davis, C. B.; Peiper, S. C.; Schall, T. J.; Littman, D. R.; Landau, N. R. *Nature* **1996**, *381*, 661; (d) Doranz, B. J.; Rucker, J.; Yi, Y. J.; Smyth, R. J.; Samson, M.; Peiper, S. C.; Parmentier, M.; Collman, R. G.; Doms, R. W. *Cell* **1996**, *85*, 1149; (e) Dragic, T.; Litwin, V.; Allaway, G. P.; Martin, S. R.; Huang, Y.; Nagashima, K. A.; Cayanan, C.; Maddon, P. J.; Koup, R. A.; Moore, J. P.; Paxton, W. A. *Nature* **1996**, *381*, 667.
4. Feng, Y.; Broder, C. C.; Kennedy, P. E.; Berger, E. A. *Science* **1996**, *272*, 872.
5. Wild, C. T.; Greenwell, T. K.; Matthews, T. J. *AIDS Res. Hum. Retroviruses* **1993**, *9*, 1051.
6. (a) Dorr, P.; Westby, M.; Dobbs, S.; Griffin, P.; Irvine, B.; Macartney, M.; Mori, J.; Rickett, G.; Smith-Burchnell, C.; Napier, C.; Webster, R.; Armour, D.; Price, D.; Stammen, B.; Wood, A.; Perros, M. *Antimicrob. Agents Chemother.* **2005**, *49*, 4721; (b) Price, D. A.; Armour, D.; De Groot, M.; Leishman, D.; Napier, C.; Perros, M.; Stammen, B. L.; Wood, A. *Bioorg. Med. Chem. Lett.* **2006**, *16*, 4633.
7. (a) Cahn, P.; Sued, O. *Lancet* **2007**, *369*, 1235; (b) Grinsztejn, B.; Nguyen, B.-Y.; Katlama, C.; Gatell, J. M.; Lazzarin, A.; Vittecoq, D.; Gonzalez, C. J.; Chen, J.; Harvey, C. M.; Isaacs, R. D. *Lancet* **2007**, *369*, 1261.
8. (a) Tamamura, H.; Xu, Y.; Hattori, T.; Zhang, X.; Arakaki, R.; Kanbara, K.; Omagari, A.; Otaka, A.; Ibuka, T.; Yamamoto, N.; Nakashima, H.; Fujii, N. *Biochem. Biophys. Res. Commun.* **1998**, *253*, 877; (b) Fujii, N.; Oishi, S.; Hiramatsu, K.; Araki, T.; Ueda, S.; Tamamura, H.; Otaka, A.; Kusano, S.; Terakubo, S.; Nakashima, H.; Broach, J. A.; Trent, J. O.; Wang, Z.; Peiper, S. C. *Angew. Chem., Int. Ed.* **2003**, *42*, 3251; (c) Tanaka, T.; Nomura, W.; Narumi, T.; Esaka, A.; Oishi, S.; Ohashi, N.; Itotani, K.; Evans, B. J.; Wang, Z.; Peiper, S. C.; Fujii, N.; Tamamura, H. *Org. Biomol. Chem.* **2009**, *7*, 3805.
9. Otaka, A.; Nakamura, M.; Nameki, D.; Kodama, E.; Uchiyama, S.; Nakamura, S.; Nakano, H.; Tamamura, H.; Kobayashi, Y.; Matsuoka, M.; Fujii, N. *Angew. Chem., Int. Ed.* **2002**, *41*, 2937.
10. (a) Zhao, Q.; Ma, L.; Jiang, S.; Lu, H.; Liu, S.; He, Y.; Strick, N.; Neamati, N.; Debnath, A. K. *Virology* **2005**, *339*, 213; (b) Schön, A.; Madani, N.; Klein, J. C.; Hubicki, A.; Ng, D.; Yang, X.; Smith, A. B., III; Sodroski, J.; Freire, E. *Biochemistry* **2006**, *45*, 10973; (c) Madani, N.; Schön, A.; Princiotto, A. M.; LaLonde, J. M.; Courter, J. R.; Soeta, T.; Ng, D.; Wang, L.; Brower, E. T.; Xiang, S.-H.; Do Kwon, Y.; Huang, C.-C.; Wyatt, R.; Kwong, P. D.; Freire, E.; Smith, A. B., III; Sodroski, J. *Structure* **2008**, *16*, 1689; (d) Haim, H.; Si, Z.; Madani, N.; Wang, L.; Courter, J. R.; Princiotto, A.; Kassa, A.; DeGrace, M.; McGee-Estrada, K.; Mefford, M.; Gabuzda, D.; Smith, A. B., III; Sodroski, J. *ProS Pathogens* **2009**, *5*, 1.
11. The structure of compound **2** was built in Sybyl and minimized with the MMFF94 force field and partial charges. (see: Halgren, T. A. *J. Comput. Chem.* **1996**, *17*, 490.) Docking was then performed using FlexSIS through its SYBYL

module, into the crystal structure of gp120 (PDB, entry 1RZJ). The binding site was defined as residues Val^{255}, Asp^{368}, Glu^{370}, Ser^{375}, Ile^{424}, Trp^{427}, Val^{430} and Val^{475}, and included residues located within a radius 4.4 Å. The ligand was considered to be flexible, and all other options were set to their default values. Figures were generated with ViewerLite version 5.0 (Accelrys Inc., San Diego, CA).

12. *For example, the synthesis of compound* **7**: To a solution of ethyl oxalyl chloride (0.400 mL, 3.48 mmol) in THF (20 mL) were added triethylamine (Et_3N) (0.480 mL, 3.48 mmol) and *p*-toluidine (373 mg, 3.48 mmol) with stirring at 0 °C. The reaction mixture was allowed to warm to room temperature, and then stirred for 6 h. After removal by filtration of the resulting salts, the filtrate was concentrated under reduced pressure. The residue was extracted with EtOAc (50 mL), and the extract was washed successively with brine (20 mL), 1 M HCl (20 mL × 2), brine (20 mL), saturated $NaHCO_3$ (20 mL × 2) and brine (20 mL × 3), then dried over $MgSO_4$. Concentration under reduced pressure gave the crude ethyl oxalamate, which was used without further purification. To a solution of the crude ethyl oxalamate (640 mg, 3.09 mmol) in THF (30 mL) were added aqueous 1 M NaOH (3.40 mL, 3.40 mmol), water (50 mL) and MeOH (20 mL) with stirring at 0 °C. The reaction mixture was allowed to warm to room temperature, and then stirred for 20 h. After the addition of aqueous 1 M HCl (5 mL), MeOH and THF were evaporated under reduced pressure. The residue was acidified to pH 2 with 1 M HCl, and extracted with EtOAc (50 mL × 2). The combined organic layer was washed with brine (20 mL × 3), and dried over $MgSO_4$. Concentration under reduced pressure gave the crude acid, which was used for the next reaction without further purification. To a solution of the above crude acid (514 mg, 2.87 mmol) in THF (10 mL) were added 1-hydoxybenzotriazole (484 mg, 3.16 mmol), 4-amino-2,2,6,6-tetramethylpiperidine (446 μL, 2.58 mmol), 1-ethyl-3-(3-dimethylaminopropyl)carbodiimide hydrochloride (606 mg, 3.16 mmol) and Et_3N (0.439 mL, 3.16 mmol) with stirring at 0 °C. The reaction mixture was allowed to warm to room temperature, and then stirred for 20 h. After evaporation of THF, the residue was dissolved in $CHCl_3$ (50 mL). The mixture was washed with saturated $NaHCO_3$ (20 mL × 2) and brine (20 mL × 3), and dried over $MgSO_4$. Concentration under reduced pressure gave the crude crystalline mass. The usual work-up followed by recrystallization from EtOAc–*n*-hexane gave the title compound **7** (363 mg, 1.14 mmol, 39.8%) as colorless crystals, mp = 176 °C; δ_H (400 MHz; $CDCl_3$) 1.07 (1H, m, NH), 1.16 (6H, s, CH_3), 1.29 (6H, s, CH_3), 1.44 (2H, m, CH_2), 1.91 (1H, d, *J* 3.7, C*H*H), 1.94 (1H, d, *J* 3.7, CH*H*), 2.34 (3H, s, CH_3), 4.25 (1H, m, CH), 7.17 (2H, d, *J* 8.3, ArH), 7.33 (1H, m, NH), 7.50 (2H, d, *J* 8.4, ArH), 9.18 (1H, s, NH); HRMS (FAB), *m*/*z* calcd for $C_{18}H_{28}N_3O_2$ $(MH)^+$ 318.2182, found 318.2173.
13. McFarland, C.; Vicic, D. A.; Debnath, A. K. *Synthesis* **2006**, 807.
14. *The synthesis of compound* **12**: To a solution of Et_3N (417 μL, 3.00 mmol) and 4-nitroaniline (138 mg, 1.00 mmol) in THF (1.3 mL) was added oxalyl dichloride (85.8 μL, 1.00 mmol) with stirring at 0 °C. After being stirred for 30 min at 0 °C, Et_3N (167 μL, 1.20 mmol) and 4-amino-2,2,6,6-tetramethylpiperidine (156 μL, 0.90 mmol) were added. The reaction mixture was stirred for 6 h at 0 °C. After removal by filtration of the resulting salts, the filtrate was concentrated under reduced pressure. The residue was dissolved in $CHCl_3$ (20 mL), and the mixture was washed successively with brine (10 mL), saturated $NaHCO_3$ (10 mL × 2) and brine (10 mL × 3), and dried over $MgSO_4$. Concentration under reduced pressure followed by flash chromatography over silica gel with $CHCl_3$–MeOH (9:1) gave 42.4 mg (0.122 mmol, 13.5%) of the title compound **12** as colorless crystals, mp = 190 °C; δ_H (400 MHz; $CDCl_3$) 1.09 (1H, m, NH), 1.17 (6H, s, CH_3), 1.29 (6H, s, CH_3), 1.43 (2H, m, CH_2), 1.92 (1H, d, *J* 3.8, C*H*H), 1.95 (1H, d, *J* 3.8, CH*H*), 4.28 (1H, m, CH), 7.29 (1H, m, NH), 7.82 (2H, d, *J* 9.1, ArH), 8.28 (2H, d, *J* 9.1, ArH), 9.55 (1H, s, NH); HRMS (FAB), *m*/*z* calcd for $C_{17}H_{25}N_4O_4$ $(MH)^+$ 349.1876, found 349.1871.
15. Yoshimura, K.; Shibata, J.; Kimura, T.; Honda, A.; Maeda, Y.; Koito, A.; Murakami, T.; Mitsuya, H.; Matsushita, S. *AIDS* **2006**, *20*, 2065.
16. (a) Chapman, N. B.; Shorter, J. *Advances in Linear Free Energy Relationship*; Plenum Press: London, 1972; (b) Chapman, N. B.; Shorter, J. *Correlation Analysis in Chemistry*: Plenum Press: London, 1978; (c) Hansch, C.; Leo, A. J.; Hoekman, D. *Exploring QSAR, Hydrophobic, Electronic, and Steric Constants*; American Chemical Society: Washington, DC, 1995.
17. Taft, R. W. In *Steric Effects in Organic Chemistry*; Newman, M. S., Ed.; John Wiley: New York, 1956; p 556.
18. (a) Chou, T. C.; Talalay, P. *J. Biol. Chem.* **1977**, *252*, 6438; (b) Chou, T. C.; Hayball, M. P. *CalcuSyn*, 2nd ed.; Biosoft: Cambridge, UK, 1996.